iScience

CellPress
OPEN ACCESS

Article

Effects of top-down influence suppression on behavioral and V1 neuronal contrast sensitivity functions in cats

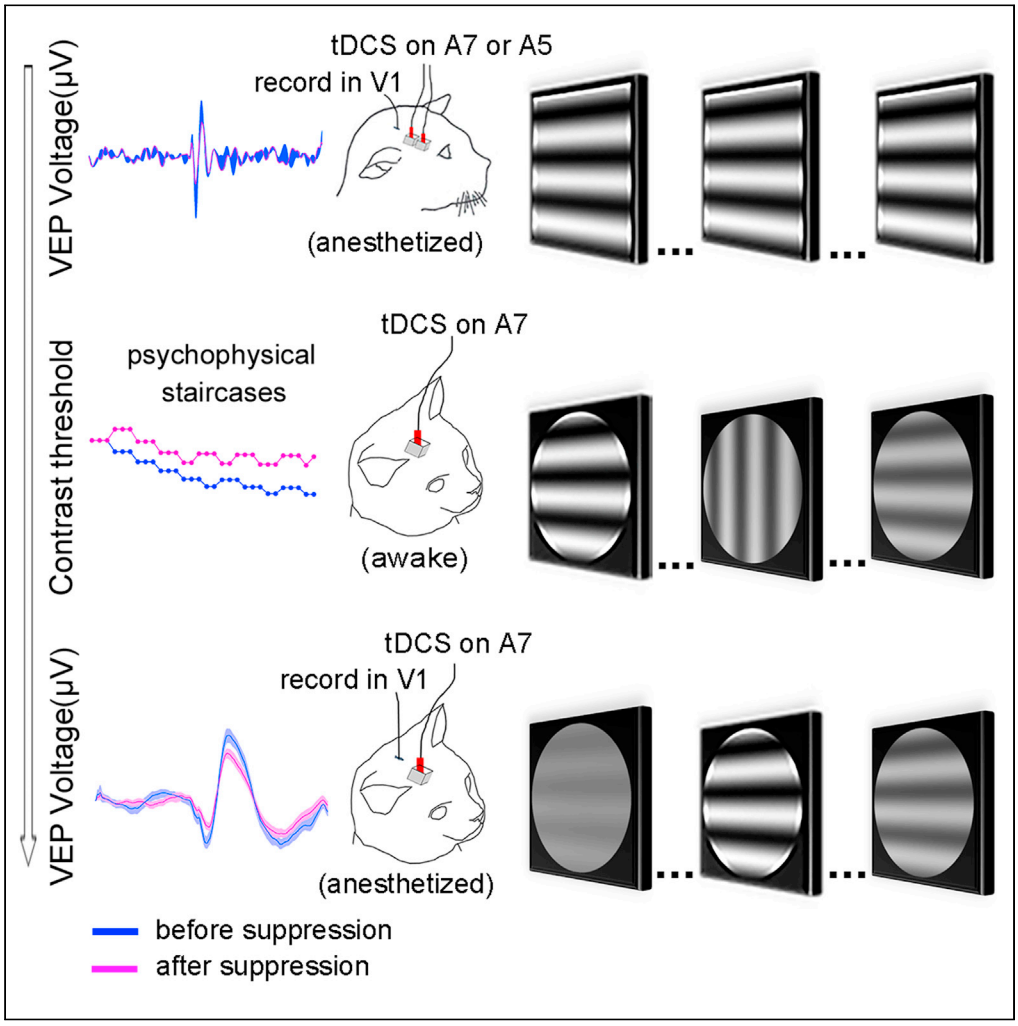

Jian Ding, Zheng Ye, Fei Xu, ..., Qingyan Sun, Tianmiao Hua, Zhong-Lin Lu

tmhua@mail.ahnu.edu.cn (T.H.)
zhonglin@nyu.edu (Z.-L.L.)

Highlights

Top-down suppression lowers both behavioral and V1 neuronal CSF functions

Top-down suppression raises both behavioral and V1 neuronal TvC functions

The neuronal CSFs and TvCs are highly correlated with their behavioral counterparts

Top-down influence lowers internal additive noise and impact of external noise in V1

Ding et al., iScience 25, 103683
January 21, 2022 © 2021 The Authors.
https://doi.org/10.1016/j.isci.2021.103683

iScience

CellPress
OPEN ACCESS

Article

Effects of top-down influence suppression on behavioral and V1 neuronal contrast sensitivity functions in cats

Jian Ding,[1,5] Zheng Ye,[1,5] Fei Xu,[1] Xiangmei Hu,[1] Hao Yu,[1] Shen Zhang,[1] Yanni Tu,[1] Qiuyu Zhang,[1] Qingyan Sun,[1] Tianmiao Hua,[1,*] and Zhong-Lin Lu[2,3,4,6,*]

SUMMARY

To explore the relative contributions of higher-order and primary visual cortex (V1) to visual perception, we compared cats' behavioral and V1 neuronal contrast sensitivity functions (CSF) and threshold versus external noise contrast (TvC) functions before and after top-down influence of area 7 (A7) was modulated with transcranial direct current stimulation (tDCS). We found that suppressing top-down influence of A7 with cathode-tDCS, but not sham-tDCS, reduced behavioral and neuronal contrast sensitivity in the same range of spatial frequencies and increased behavioral and neuronal contrast thresholds in the same range of external noise levels. The neuronal CSF and TvC functions were highly correlated with their behavioral counterparts both before and after the top-down suppression. Analysis of TvC functions using the Perceptual Template Model (PTM) indicated that top-down influence of A7 increased both behavioral and V1 neuronal contrast sensitivity by reducing internal additive noise and the impact of external noise.

INTRODUCTION

Visual perception is accomplished through information processing in a network with feedforward, feedback, and recurrent connections (Angelucci et al., 2017; Angelucci and Bressloff, 2006; Federer et al., 2021; Merrikhi et al., 2018). Most studies have focused on the primary visual cortex (V1), where neurons exhibit response sensitivities comparable to behavioral performance in visual signal detection (Barlow et al., 1987; Busse et al., 2011; Chirimuuta and Tolhurst, 2005; Glickfeld et al., 2013; Meng et al., 2013; Niemeyer and Paradiso, 2016; Parisi et al., 2006; Ress and Heeger, 2003), and information processing along feedforward connections from low- to high-level visual cortical areas (Dreher et al., 1996; Hubel and Wiesel, 1968; Lee, 2002; Nassi and Callaway, 2009). However, there is mounting evidence suggesting that top-down feedback affects neural processing (Gilbert and Li, 2013). How top-down influence affects visual perception at the behavioral level and neuronal processing in low-level visual areas is less well understood. Numerous physiological studies have shown that neuronal responses in the low-level visual areas can be altered when higher-order visual areas are affected by pharmacological administration (Chen et al., 2014; Hishida et al., 2019; Tong et al., 2011; Yang et al., 2016b), cooling (Huang et al., 2017; Nassi et al., 2013; Wang et al., 2000, 2007, 2010), optogenetic manipulation (Huh et al., 2018; Keller et al., 2020; Nurminen et al., 2018; Pafundo et al., 2016; Pak et al., 2020; Zhang et al., 2014), and attention (Chalk et al., 2010; Lee and Maunsell, 2010; Li et al., 2008; Lu et al., 2011; Thiele et al., 2009; Williford and Maunsell, 2006), but the results are diverse or even contradictory (Han and VanRullen, 2016; Harrison et al., 2007; Hishida et al., 2019; Huh et al., 2018; Lu et al., 2011; Murray et al., 2002; Nassi et al., 2013; Tong et al., 2011; Wang et al., 2000, 2007; Zhang et al., 2014), probably because different modulation techniques might have caused variations in the time course and reversibility of top-down effects. Furthermore, these studies have not examined behavioral changes after acute modification of top-down influence (Zhang et al., 2014). Conversely, other studies have evaluated top-down influence on behavioral performance but have not examined its influence on neuronal processing in low-level cortical areas (Cutrone et al., 2014; Dosher and Lu, 2000a; b; Lu and Dosher, 1998, 2004; Rolls, 2008; Schweid et al., 2008). Therefore, it remains unclear how top-down influence affects both visual detection behavior and neuronal processing in low-level cortical areas.

The goal of this study is to investigate effects of top-down influence of area 7 (A7) on V1 (area 17) neuronal processing and its potential causal effects on contrast detection behavior by modulating neuronal activity

[1]College of Life Sciences, Anhui Normal University, Wuhu, Anhui 241000, China

[2]Divison of Arts and Sciences, NYU Shanghai, Shanghai 200122, China

[3]Center for Neural Science and Department of Psychology, New York University, New York, NY 10003, USA

[4]NYU-ECNU Institute of Brain and Cognitive Science, NYU Shanghai, Shanghai 200062, China

[5]These authors contributed equally

[6]Lead contact

*Correspondence: tmhua@mail.ahnu.edu.cn (T.H.), zhonglin@nyu.edu (Z.-L.L.)

https://doi.org/10.1016/j.isci.2021.103683

This is an open access article under the CC BY-NC-ND license (http://creativecommons.org/licenses/by-nc-nd/4.0/).

in A7 with transcranial direct current stimulation (tDCS). In addition, we applied the external noise paradigm and Perceptual Template Model (PTM) analysis to reveal mechanisms of top-down influence on neuronal and behavioral functions.

Located on the middle suprasylvian gyrus and the adjacent lateral bank of the lateral sulcus, the A7 receives input neural connectivity from area 19, 20a, 20b, 21a, 21b, AMLS, ALLS, and PLLS (Connolly et al., 2012; Olson and Lawler, 1987). Based on its location and neural connectivity pattern, it is defined as a higher-order extrastriate visual cortical area (Hicks et al., 1988). Recent studies using neural tracing with horseradish peroxidase (HRP) showed that A7 had direct feedback connections to area 17 of the primary visual cortex (V1), and the feedback neurons are primarily pyramidal cells that are distributed in discontinuous and sequential patches in layers 1, 2, and 3 or layer 5 of A7 (Han et al., 2008; Yang et al., 2016b). Studies using fMRI have found that inactivation of A7 with local injection of GABA or lesion induced by liquid nitrogen freezing caused a spatial frequency-dependent decrease in response amplitude of orientation maps in both area 17 and 18 (Yang et al., 2016b). The evidence indicates that A7 is a high-level visual cortical area that may have direct excitatory top-down influence on low-level cortical areas. Nevertheless, how feedback from A7 affects behavioral and V1 neuronal contrast sensitivity functions remains unclear.

tDCS is a widely used noninvasive tool that can reversibly modulate neuronal excitability in the stimulated local brain region (Impey et al., 2016; Krause et al., 2013; Kunori and Takashima, 2019; Nitsche and Paulus, 2000; Pan et al., 2021a; Zhao et al., 2020). Because tDCS-induced effects can last for 60–90 min (Bachtiar et al., 2015; Monte-Silva et al., 2010; Nitsche and Paulus, 2001; Schweid et al., 2008; Stagg et al., 2009, 2011; Zhao et al., 2020), it gives us enough time to measure top-down influence on neuronal contrast sensitivity functions and animal behavioral performance in contrast detection.

The PTM was constructed to model observer performance in perceptual tasks in terms of perceptual template(s), transducer nonlinearity, and internal additive and multiplicative noises (Dosher and Lu, 1999; Lu and Dosher, 1998). It has been used to identify mechanisms of attention (Dosher and Lu, 2000a; Lu and Dosher, 1998, 2004) and perceptual learning (Dosher and Lu, 1999; Huang et al., 2008; Lu et al., 2005; Zhou et al., 2006). In this study, we applied the external noise paradigm to measure both behavioral and neuronal TvC functions and the PTM to identify mechanisms underlying effects of top-down suppression.

The experiments were conducted on three cats after successful conditioning training. We measured the behavioral CSF in zero external noise, and the TvC function in detecting a grating stimulus at a fixed SF, as well as visually evoked field potentials (VEPs) from V1 before and after tDCS of A7. Neuronal CSF and TvC functions were constructed based on Receiver Operating Characteristics (ROC) analysis. We found that suppressing top-down influence of A7 with cathode (c)-tDCS, but not sham (s)-tDCS, significantly decreased both behavioral and neuronal contrast sensitivities (CS) in the same range of spatial frequencies (SFs) and significantly increased both the behavioral and neuronal contrast thresholds over the same range of external noise levels. The neuronal CSF and TvC were highly correlated with their behavioral counterparts both before and after suppression of the top-down influence. Analysis of the TvC functions with the PTM indicated that suppression of top-down influence increased internal additive noise and the impact of external noise at both the behavioral and neuronal levels. Taken together, these results suggest that top-down influence of A7 increases both behavioral and V1 neuronal contrast sensitivity by reducing internal additive noise and the impact of external noise.

RESULTS

Top-down influence of A7 on neuronal activity in the V1 cortex

To confirm whether top-down influence of A7 affected neuronal activity in V1, we recorded VEPs from V1 of four cats before and at different time points (0–90 min with an interval of 10 min) after the end of sham (s)- and cathode (c)-tDCS in A7 as well as c-tDCS in area 5 (A5), a nonvisual cortical area adjacent to A7 (Avendaño et al., 1988; Galuske et al., 2002; Han et al., 2008; Lajoie et al., 2010; Olausson et al., 1990; Wong et al., 2018) (See STAR Methods) (Figures 1A–1C). The VEP traces contained an initial negative N1 component, a positive P1 component, and a late negative N2 component, consistent with previous studies (Aydin-Abidin et al., 2006; Padnick and Linsenmeier, 1999; Tomiyama et al., 2016; Zhao et al., 2020). The latencies of the N1, P1, and N2 components in V1 were 24.1–38.8, 49.4–72.5, and 105.6–139.5 ms after the stimulus onset, evidently shorter than those in visual cortical area 21a (Zhao et al., 2020).

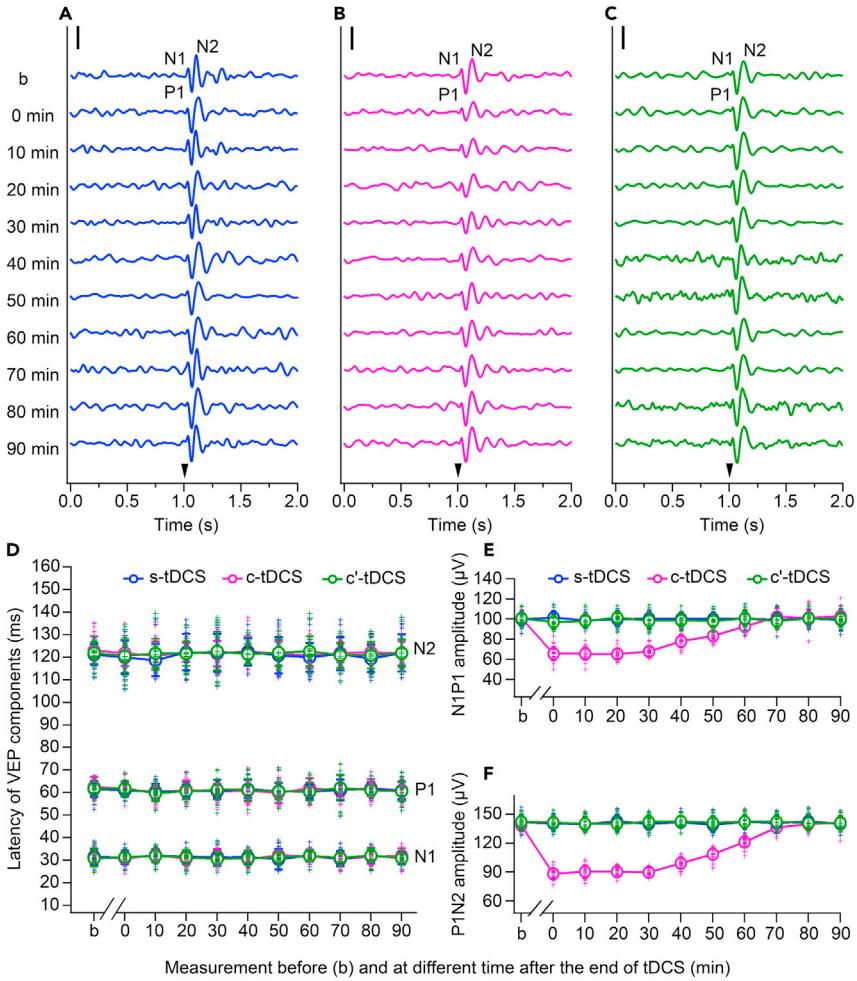

Figure 1. Top-down influence of A7 on the VEPs in V1

(A–C) Sample VEP voltage traces showing the three main components (N1, P1, and N2) as well as the changes of VEPs before (b) and at different time points (0, 10, 20, 30, 40, 50, 60, 70, 80, and 90 min) after sham (s)-tDCS in A7, cathode (c)-tDCS in A7, and c-tDCS in A5 (c′-tDCS), respectively. Solid arrowheads indicate visual stimulus onsets. The vertical solid scale bars in the upper left corners represent 100 μV.

(D) The mean latency (blue, magenta, and green open circles with error bar of SDs) at the peak of the N1, P1, and N2 components across 4 cats before (b) and at different time points (0–90 min) after s-tDCS in A7 (blue), c-tDCS in A7 (magenta), and c-tDCS in A5 (c′-tDCS) (green), respectively. The blue, magenta, and green crosses represent individual data points of 24 measurements across 4 cats before and after s-tDCS in A7, c-tDCS in A7, and c-tDCS in A5, respectively.

(E and F) The peak-to-peak amplitude of N1P1 (E) and P1N2 (F) complexes across all cats before (b) and at different time points (0–90 min) after the end of tDCS. The blue, magenta, and green open circles indicate the mean amplitude (means ± SDs) measured at each time point before and after s-tDCS in A7, c-tDCS in A7, and c-tDCS in A5, respectively. The blue, magenta, and green crosses represent individual data points of 24 measurements across 4 cats (6 repeated measurements/cat) before and after s-tDCS in A7, c-tDCS in A7, and c-tDCS in A5, respectively.

The mean latency of the N1, P1, and N2 components in V1 across all cats showed no significant effect of measurement time (0, 10, 20, 30, 40, 50, 60, 70, 80, and 90 min) after s- and c-tDCS in A7 as well as c-tDCS in A5 (N1: $F(10,759) = 1.63$, $p = 0.094$; P1: $F(10,759) = 1.563$, $p = 0.113$; N2: $F(10,759) = 0.721$, $p = 0.705$), with no significant interaction between measurement time and tDCS condition (N1: $F(20, 759) = 0.678$, $p = 0.85$; P1: $F(20, 759) = 0.437$, $p = 0.985$; N2: $F(20, 759) = 0.438$, $p = 0.985$) (Figure 1D), suggesting that tDCS in A7 and A5 had no significant impact on the latencies of VEP components in V1.

The peak-to-peak amplitudes of the N1P1 and P1N2 complexes were extracted and analyzed (Aydin-Abidin et al., 2006; Souza et al., 2007; Zhao et al., 2020). Two-way ANOVA indicated that N1P1 and P1N2

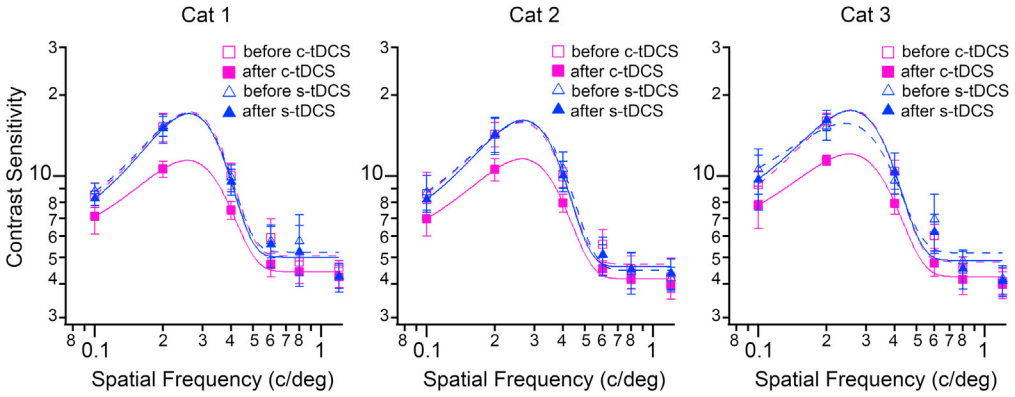

Figure 2. Behavioral contrast sensitivity functions measured in three cats (Cat1, Cat2, and Cat3) before (open symbol) and after (filled symbol) sham (s)-tDCS (blue triangle) and cathode (c)-tDCS (magenta square) in A7, respectively

The behavioral contrast sensitivity was the inverse of threshold contrast needed for detecting visual stimuli at different spatial frequencies. The dotted (before tDCS) and solid (after tDCS) curves in each plot represent the best gauss fits of contrast sensitivity functions. Error bars stand for SDs computed from multiple trials.

amplitudes measured before and at different time points after s- and c-tDCS in A7 as well as c-tDCS in A5 showed a significant main effect of time (N1P1: $F(10,759) = 52.193$, $p < 0.0001$; P1N2: $F(10,759) = 107.77$, $p < 0.0001$) and interaction between time and tDCS condition (N1P1: $F(20,759) = 48.402$, $p < 0.0001$; P1N2: $F(20,759) = 101.488$, $p < 0.0001$) (Figures 1E and 1F). Additional one-way ANOVA showed that the mean N1P1 and P1N2 amplitudes before and after s-tDCS in A7 did not significantly vary with time (N1P1: $F(10,253) = 0.316$, $p = 0.976$; P1N2: $F(10,253) = 0.825$, $p = 0.604$) and c-tDCS in A5 (N1P1: $F(10,253) = 1.142$, $p = 0.331$; P1N2: $F(10,253) = 0.395$, $p = 0.948$), but the mean N1P1 and P1N2 amplitudes before and after c-tDCS in A7 varied significantly with time (N1P1: $F(10,253) = 153.474$, $p < 0.0001$; P1N2: $F(10,253) = 405.723$, $p < 0.0001$) (Figures 1E and 1F). More specifically, post hoc analysis indicated that the mean N1P1 and P1N2 amplitudes at 0, 10, 20, 30, 40, 50, and 60 min after c-tDCS in A7 were significantly lower than those before c-tDCS (N1P1: all $p < 0.0001$; P1N2: all $p < 0.0001$), whereas the mean N1P1 and P1N2 amplitudes at 70, 80, and 90 min after c-tDCS did not differ significantly from those before c-tDCS (N1P1: $p = 0.444$, 0.748, and 0.244; P1N2: $p = 0.141$, 0.48 and 0.087) (Figures 1E–1F).

These results demonstrated that c-tDCS in A7, but not s-tDCS, suppressed neuronal excitability in V1, and the effect lasted about 60–70 min. The c-tDCS-induced VEP amplitude reduction in V1 reflected top-down influence of A7, not direct current stimulation across cortical regions, because c-tDCS in the adjacent nonvisual A5 exhibited no significant influence on VEP amplitudes in V1.

Top-down influence on behavioral and neuronal CSFs

To examine how top-down influence affects behavioral contrast sensitivity and neuronal contrast sensitivity in V1, we measured both behavioral and neuronal CSF functions in three cats after conditioning training (see STAR Methods).

Top-down influence on behavioral CSF

We measured behavioral CSF at 79.4% correct performance level before and after tDCS in A7 using a 3-down/1-up staircase method (see STAR Methods, Figure S1, Video S1). As shown in Figure 2, the behavioral CSFs had an inverted-U shape for all three cats, with peaks between 0.2 and 0.4 cycle/deg. A two-factor ANOVA across three cats showed that c-tDCS in A7 had a significant effect on contrast sensitivity (CS) ($F(1,276) = 256.362$, $p < 0.0001$) and a significant interaction with SF ($F(5,276) = 34.861$, $p < 0.0001$) (Figure 2). Post hoc analysis showed that c-tDCS significantly reduced CS at 0.1, 0.2, 0.4, and 0.6 cycle/deg (all $p < 0.0001$), but had no significant effect on CS at 0.8 ($p = 0.123$) and 1.2 ($p = 0.35$) cycle/deg. By contrast, s-tDCS had no significant effect on the CS ($F(1,276) = 1.286$, $p = 0.258$) and no interaction with SF ($F(5,276) = 0.565$, $p = 0.727$) (Figure 2). These results demonstrated that c-tDCS in A7 reduced behavioral contrast sensitivity in low and intermediate SFs (0.1–0.6 cycle/deg).

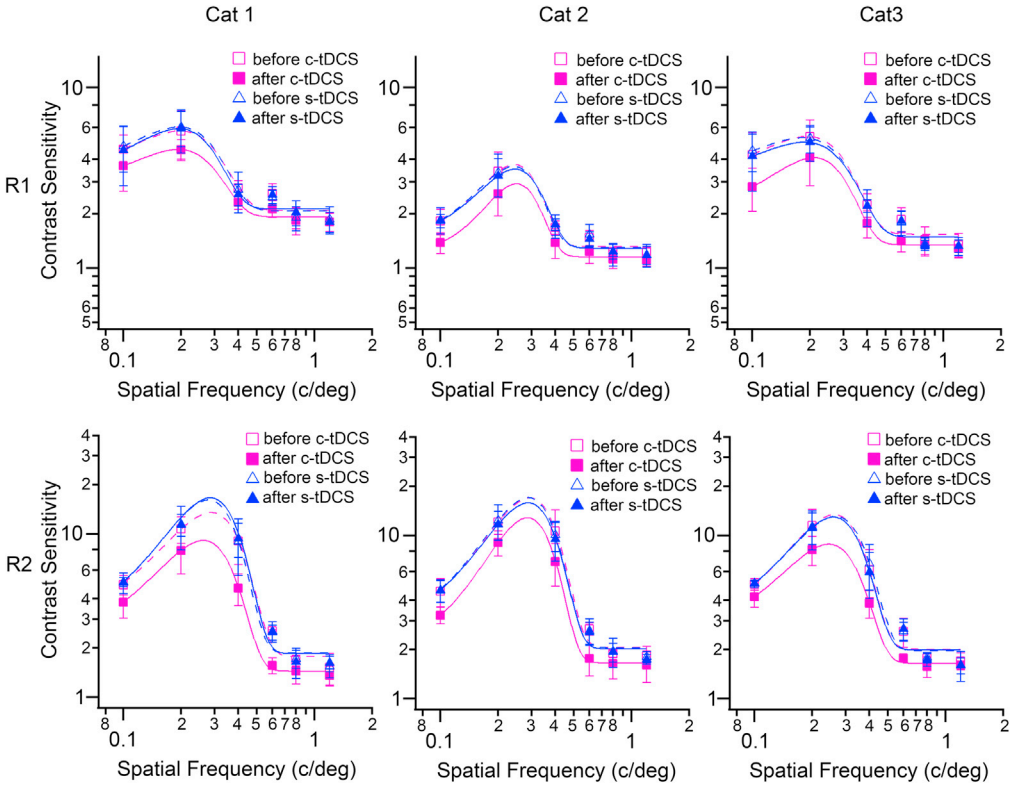

Figure 3. Neuronal contrast sensitivity functions in three cats (Cat1, Cat2, and Cat3) before (open symbol) and after (filled symbol) sham (s)-tDCS (blue triangle) and cathode (c)-tDCS (magenta square) in A7, respectively

The neuronal contrast sensitivity was the inverse of threshold contrast measured by ROC analysis of N1P1 (R1) and P1N2 (R2) amplitudes recorded in V1. The dotted (before tDCS) and solid (after tDCS) curves in each plot represent the best gauss fits of contrast sensitivity functions. Error bars stand for SDs.

Top-down influence on neuronal CSF

We estimated neuronal CSFs at the 79.4% accuracy level based on ROC analysis of the N1P1 and P1N2 amplitudes of VEPs recorded from V1 before and after tDCS in A7 (see STAR Methods, Figures S2, S3). Similar to the behavioral CSFs, the neuronal CSFs had an inverted U-shape, with peaks between SF 0.2 and 0.4 cycle/deg (Figure 3). A two-factor ANOVA across three cats showed that c-tDCS in A7 had a significant effect on both N1P1- and P1N2-neuronal CS (N1P1: $F(1,708) = 55.814$, $p < 0.0001$; P1N2: $F(1,708) = 186.202$, $p < 0.0001$) and a significant interaction with SF (N1P1: $F(5,708) = 7.073$, $p < 0.0001$; $F(5,708) = 28.945$, P1N2: $p < 0.0001$) (Figure 3). Post hoc analysis showed that c-tDCS in A7 significantly reduced CS at 0.1, 0.2, 0.4, and 0.6 cycle/deg (N1P1: all $p < 0.02$; P1N2: all $p < 0.002$), but had no significant effect on CS at 0.8 (N1P1: $p = 0.61$; P1N2: $p = 0.389$) and 1.2 cycle/deg (N1P1: $p = 0.694$; P1N2: $p = 0.542$) (Figure 3). By contrast, s-tDCS had no significant effect on the N1P1- and P1N2-neuronal CS (N1P1: $F(1,708) = 0.596$, $p = 0.441$; P1N2: $F(1,708) = 0.425$, $p = 0.515$) and no interaction with SF (N1P1: $F(5,708) = 0.275$, $p = 0.927$; P1N2: $F(5,708) = 0.177$, $p = 0.971$) (Figure 3). These results demonstrated that c-tDCS in A7 reduced neuronal contrast sensitivity in low and intermediate SFs (0.1–0.6 cycle/deg).

In summary, c-tDCS in A7 reduced both behavioral and V1-neuronal CSFs in the same SF range. To further examine the relationship between these two effects, we analyzed the correlation between behavioral and neuronal CSFs before and after c-tDCS in A7. Before c-tDCS, the behavioral CSFs were significantly correlated with neuronal CSFs constructed from N1P1 (mean $r^2 = 0.912$, $p = 0.011$) and P1N2 (mean $r^2 = 0.977$, $p = 0.001$) (Figure 4A and 4B). After c-tDCS, the behavioral CSFs were also significantly correlated with the N1P1-neuronal CSFs (mean $r^2 = 0.923$, $p = 0.009$) and P1N2-neuronal CSFs (mean $r^2 = 0.99$, $p < 0.0001$) (Figures 4C and 4D).

c-tDCS in A7 reduced the mean behavioral CS by 16.43%, 27.17%, 22.14%, and 18.17% at 0.1, 0.2, 0.4, and 0.6 cycle/deg, respectively, the mean N1P1-neuronal CS by 21.99%, 18.14%, 17.82%, and 18.15%, and the

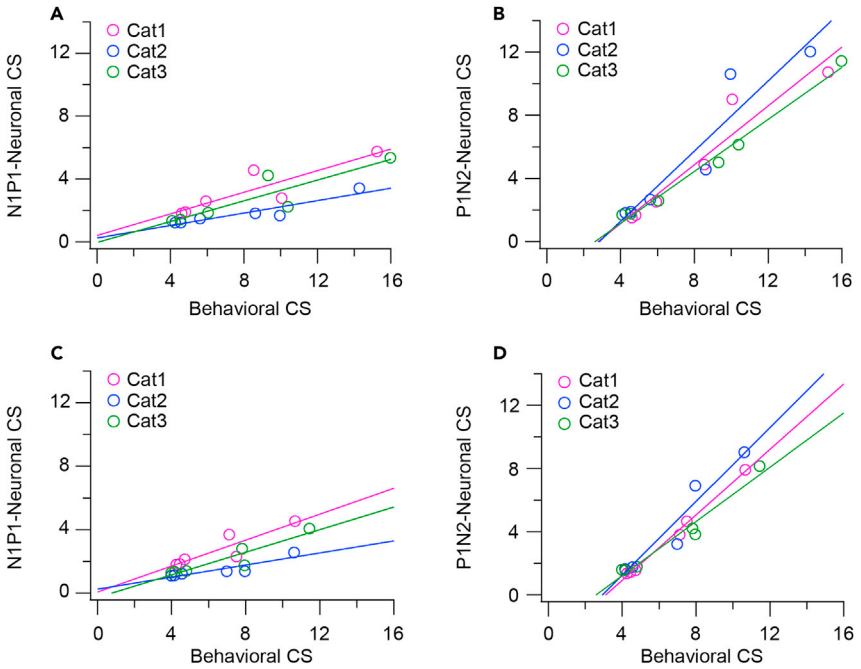

Figure 4. Correlation between behavioral and neuronal contrast sensitivity at different spatial frequencies

Scatterplots of neuronal versus behavioral contrast sensitivities at different spatial frequencies (0.1, 0.2, 0.4, 0.6, 0.8, and 1.2 cpd) for three cats (Cat1, Cat2, and Cat3) before (A and B) and after (C and D) c-tDCS in A7. The magenta, blue, and green open circles represent neuronal and behavioral contrast sensitivity (CS) in Cat1, Cat2, and Cat3, respectively. The magenta, blue, and green solid lines in each plot represent the best linear fits.

mean P1N2-neuronal CS by 23.71%, 41.43%, 41.91%, and 35.92% at 0.1, 0.2, 0.4, and 0.6 cycle/deg, respectively. ANOVA analysis showed that the behavioral CS reductions at 0.1, 0.2, 0.4, and 0.6 cycle/deg were not significantly different from the N1P1-neuronal CS reductions ($F(1,328) = 0.850$, $p = 0.357$) but significantly lower than the P1N2-neuronal CS reductions ($F(1,328) = 51.799$, $p < 0.0001$) with no significant interaction with SF ($F(3,328) = 1.761$, $p = 0.154$). The results suggested that neuronal contrast sensitivities measured with the earlier VEP components (N1P1) in V1 were similarly affected by A7 top-down influence as the behavioral contrast sensitivities, whereas the neuronal contrast sensitivities measured with the later VEP components (P1N2) in V1 were more sensitive to A7 top-down influence than behavioral contrast sensitivities.

Mechanisms of top-down influence on visual contrast sensitivity

Comparisons of post- and pre-tDCS TvC functions

To identify the mechanisms of top-down influence on visual contrast sensitivity, we measured the behavioral and neuronal threshold versus external noise contrast (TvC) functions in the three trained cats. The behavioral TvC functions of the cats, measured at 70.7% (using a 2-down/1-up staircase) and 79.4% correct (using a 3-down/1-up staircase) performance criteria (see STAR Methods, Figure S1, Video S2), were similar in shape to those of human subjects (Dosher and Lu, 1999; Huang et al., 2009; Lu and Dosher, 1998, 2008; Zhou et al., 2006): the log threshold contrast (TC) values were relatively constant in low external noise conditions, but increased linearly with log external noise contrast in high external noise conditions (Figure 5). A three-factor ANOVA showed that c-tDCS in A7 significantly increased the behavioral TCs ($F(1,340) = 282.022$, $p < 0.0001$), with no significant interaction with external noise level ($F(4,340) = 0.113$, $p = 0.978$) and performance criterion ($F(1,340) = 1.773$, $p = 0.184$) (Figure 5). By contrast, s-tDCS in A7 had no significant effect on the behavioral TCs ($F(1,340) = 0.243$, $p = 0.622$) (Figure 5).

The neuronal TvC functions were estimated at the 70.7% and 79.4% accuracy levels based on ROC analyses of the VEPs recorded in V1 before and after tDCS in A7 (see STAR Methods). The shapes of the neuronal TvC functions constructed from N1P1 and P1N2 were similar to that of the behavioral TvC functions

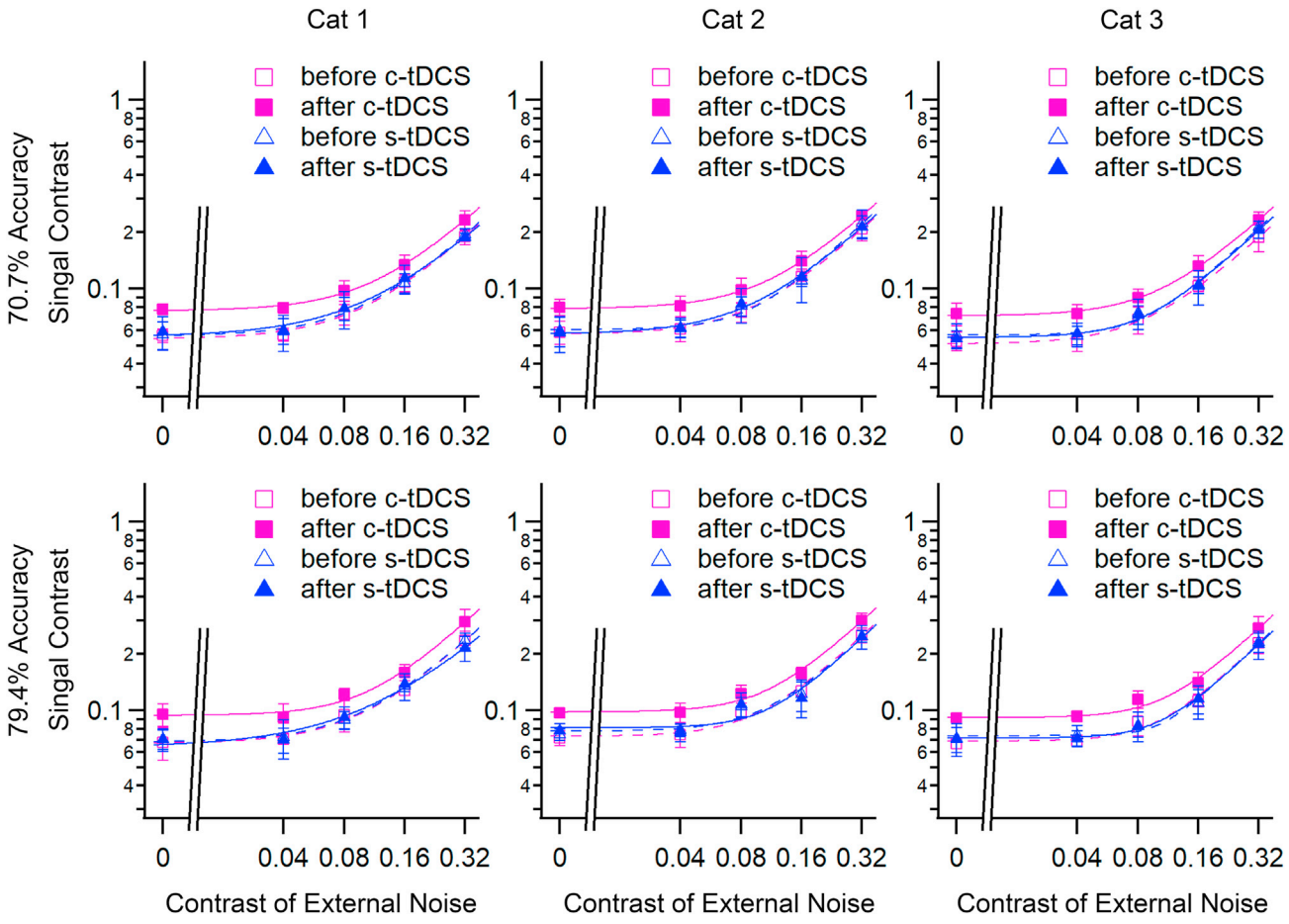

Figure 5. Behavioral contrast threshold versus external noise contrast (TvC) functions

Behavioral TvC functions measured at two performance levels (70.7% and 79.4% accuracy) in three cats (Cat1, Cat2, and Cat3) before (open symbol) and after (filled symbol) s-tDCS (blue triangle) and c-tDCS (magenta square) in A7, respectively. The dotted (before tDCS) and solid (after tDCS) curves represent the best Perceptual Template Model (PTM) fits of TvC functions. Error bars stand for SDs.

(Figure 6). Three-factor ANOVA indicated that c-tDCS in A7 significantly increased the N1P1- and P1N2-neuronal TCs (N1P1: $F(11,180) = 183.441$, $p < 0.0001$; P1N2: $F(11,180) = 294.671$, $p < 0.0001$), with no significant interaction with external noise level (N1P1: $F(41,180) = 1.730$, $p = 0.141$; P1N2: $F(41,180) = 0.10$, $p = 0.982$) and performance criterion (N1P1: $F(11,180) = 0.375$, $p = 0.827$; P1N2: $F(11,180) = 0.437$, $p = 0.509$) (Figure 6). By contrast, s-tDCS in A7 had no significant effect on N1P1- and P1N2-neuronal TCs (N1P1: $F(11,180) = 1.493$, $p = 0.222$; P1N2: $F(11,180) = 0.097$, $p = 0.755$) (Figure 6).

In summary, c-tDCS in A7 had similar effects on both behavioral and V1-neuronal TvC functions, and the effects were independent of external noise level and performance criterion. To further examine the relationship of the effects, we analyzed the correlation between behavioral and neuronal TvC functions before and after c-tDCS in A7. Before c-tDCS, the behavioral TvCs were highly correlated with N1P1-neuronal TvCs at both the 70.7% (mean $r^2 = 0.999$, $p < 0.0001$) and 79.4% (mean $r^2 = 0.992$, $p = 0.001$) performance levels and the P1N2-neuronal TvCs at both the 70.7% (mean $r^2 = 0.994$, $p = 0.001$) and 79.4% (mean $r^2 = 0.986$, $p = 0.002$) performance levels (Figure 7). After c-tDCS in A7, the behavioral TvCs were also highly correlated with N1P1-neuronal TvCs at both the 70.7% (mean $r^2 = 0.999$, $p < 0.0001$) and 79.4% (mean $r^2 = 0.994$, $p = 0.001$) performance levels and the P1N2-neuronal TvCs at both the 70.7% (mean $r^2 = 0.995$, $p < 0.0001$) and 79.4% (mean $r^2 = 0.986$, $p = 0.002$) performance levels (Figure 7).

c-tDCS in A7 increased the average behavioral TC by 38.29%, 38.43%, 33.45%, 24.74%, and 21.22% at the 70.7% performance level and by 40.80%, 35.07%, 29.67%, 24.73%, and 20.42% at the 79.4% performance

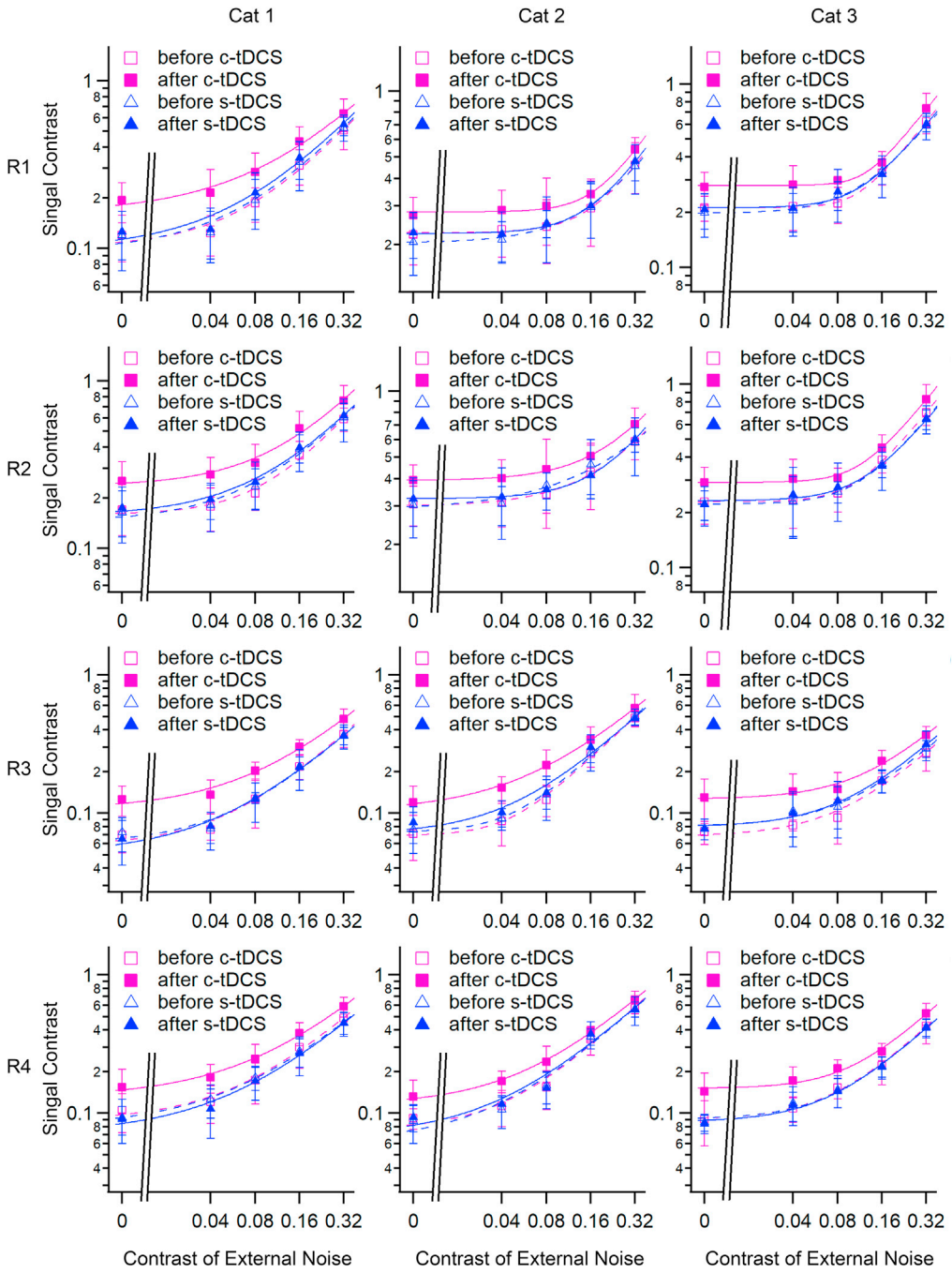

Figure 6. Neuronal contrast threshold versus external noise contrast (TvC) functions

Neuronal TvC functions constructed based on N1P1 (R1, R2) and P1N2 (R3, R4) amplitude at 70.7% (R1, R3) and 79.4% (R2, R4) performance levels before (open symbol) and after (filled symbol) s-tDCS (blue triangle) and c-tDCS (magenta square) in A7, respectively. The dotted (before tDCS) and solid (after tDCS) curves represent the best PTM fits of TvC functions. Error bars stand for SDs.

level in the 0.00, 0.04, 0.08, 0.16, and 0.32 external noise contrast conditions, respectively. In comparison, c-tDCS in A7 increased the average N1P1-neuronal TC by 46.89%, 56.72%, 46.11%, 30.45%, and 26.65% at the 70.7% performance level and by 44.71%, 48.51%, 45.16%, 34.27%, and 24.76% at the 79.4% performance level in the 0.00, 0.04, 0.08, 0.16, and 0.32 external noise contrast conditions, respectively. c-tDCS in A7 increased the average P1N2-neuronal TC across by 98.67%, 121.53%, 83.05%, 41.03%, and 32.76% at the

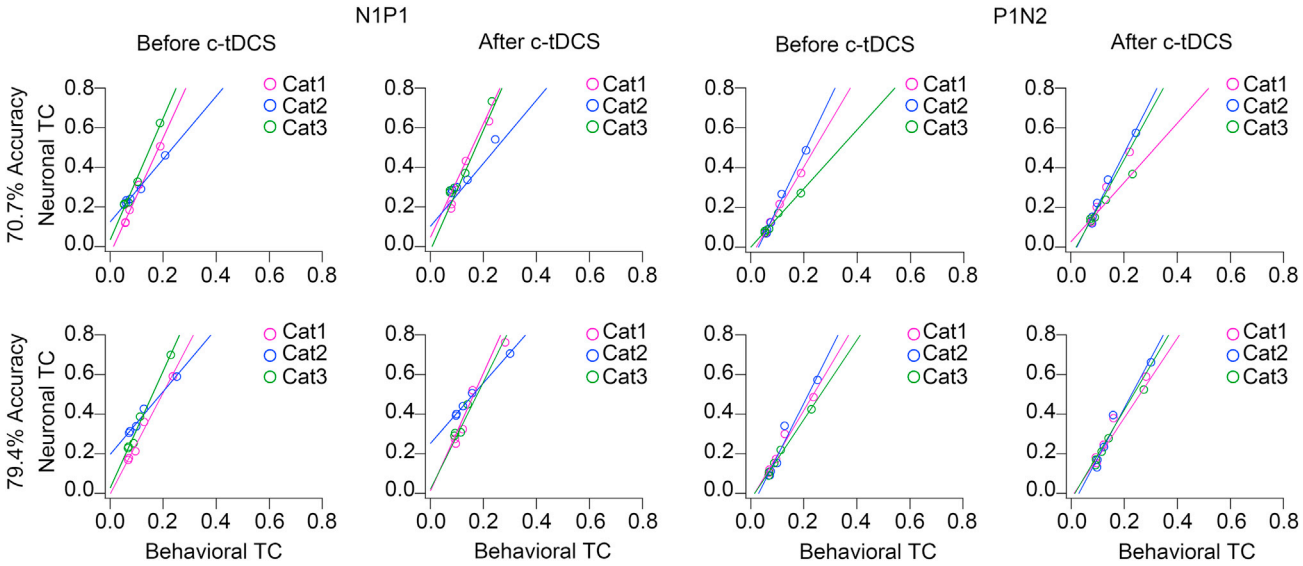

Figure 7. Correlation between behavioral and neuronal threshold contrast (TC) at different external noise level

Scatterplots of neuronal versus behavioral TCs at different external noise level (0.00, 0.04, 0.08, 0.16, and 0.32) for three cats (Cat1, Cat2, and Cat3) before and after c-tDCS in A7. The magenta, blue, and green solid lines in each plot represent the best linear fits.

70.7% performance level and by 57.61%, 65.04%, 58.16%, 32.88%, and 22.62% at the 79.4% performance level in the 0.00, 0.04, 0.08, 0.16, and 0.32 external noise contrast conditions, respectively. ANOVA showed that the average behavioral TC increases were not significantly different from the average N1P1-neuronal TC increases at both the 70.7% ($F(1,380) = 2.661$, $p = 0.104$) and 79.4% ($F(1,380) = 2.550$, $p = 0.111$) performance levels, but were significantly lower than the P1N2-neuronal TC increases at both the 70.7% ($F(1,380) = 11.136$, $p = 0.001$) and 79.4% ($F(1,380) = 8.387$, $p = 0.004$) performance levels with no significant interaction with noise contrast condition (70.7%: $F(4,380) = 0.778$, $p = 0.54$; 79.4%: $F(4,380) = 0.847$, $p = 0.496$). These results indicated that the behavioral and neuronal TCs measured with the early VEP components (N1P1) in V1 were comparably affected by A7 top-down influence, but neuronal TCs measured by the later VEP components (P1N2) were more susceptible to A7 top-down influence than behavioral TCs, consistent with results on behavioral and neuronal CSFs.

PTM modeling analysis

To detect the mechanism of top-down influence at a system level, we fit the PTM to the behavioral and neuronal TvC functions (see STAR Methods). For all subjects and their average, the best fitting model to the behavioral TvC function (r^2>0.97) consisted of a mixture of two mechanisms (Table 1): stimulus suppression (as indicated by an A_a of 1.769 $\pm$ 0.332) and increased external noise admission (as indicated by an A_f of 1.189 $\pm$ 0.126). This model was statistically equivalent to the most saturated model with three mechanisms (all $p > 0.5$, Table 1) and was superior to all its reduced models (all $p < 0.05$, Table 2).

Similar results were obtained on the neuronal TvC functions. For all subjects and their average, the best fitting model ($r^2 > 0.96$) to both the N1P1- and P1N2-neuronal TvC functions also consisted of a mixture of two mechanisms (Table 1): stimulus suppression (as indicated by an A_a of 1.963 $\pm$ 0.348) and increased external noise admission (as indicated by an A_f of 1.291 $\pm$ 0.064). This model was statistically equivalent to the most saturated model with three mechanisms (all $p > 0.4$, Table 1) and was superior to all its reduced models (all $p < 0.05$, Table 2).

As shown earlier, top-down suppression of A7 exerted similar effects on behavioral and neuronal TvC functions measured with the early VEP components (N1P1) in V1; we also fit a single PTM to both the behavioral and N1P1-neuronal TvC functions. Because the neuronal TC were evidently higher than the corresponding behavioral TC both before and after top-down influence suppression (Figures 5 and 6), we added a parameter A to normalize the neuronal template gain relative to the behavioral template gain in the PTM by multiplying β with A in Equation 1. Again, for all subjects and their average, the best fitting model to the behavioral and neuronal TvC

Table 1. The best-fitting parameters (mean ± SD) of the Perceptual Template Model (PTM) to the behavioral and neuronal TvC functions in each cat (Cat1, Cat2, and Cat3) and their average (Cat1–3) before and after top-down influence was suppressed by c-tDCS in A7

TvC functions	Fitting parameter	Cat1	Cat2	Cat3	Cat1-3
Behavioral	N_a	0.042±0.017	0.019±0.012	0.021±0.015	0.022±0.016
	N_m	0.086±0.113	0.052±0.039	0.055±0.039	0.055±0.040
	β	2.007±0.031	1.640±0.131	1.847±0.165	1.748±0.155
	γ	1.437±0.218	1.757±0.273	1.737±0.300	1.718±0.301
	A_a	1.583±0.244	1.736±0.290	1.790±0.305	1.769±0.332
	A_f	1.269±0.124	1.186±0.093	1.225±0.124	1.189±0.126
	r^2	0.971	0.983	0.983	0.983
	p	0.9993	0.560	1.000	1.000
N1P1-neuronal	N_a	0.034±0.031	0.095±0.098	0.009±0.011	0.041±0.037
	N_m	0.074±0.030	0.230±0.228	0.076±0.029	0.074±0.031
	β	0.708±0.131	0.973±0.314	0.565±0.056	0.693±0.140
	γ	1.514±0.435	1.775±0.779	2.227±0.300	1.713±0.539
	A_a	2.219±1.008	1.444±0.353	1.868±0.631	1.921±0.925
	A_f	1.349±0.255	1.261±0.277	1.177±0.145	1.256±0.285
	r^2	0.967	0.990	0.989	0.985
	p	0.820	0.998	1.000	0.439
P1N2-neuronal	N_a	0.045±0.032	0.014±0.015	0.044±0.032	0.032±0.030
	N_m	0.060±0.122	0.078±0.030	0.067±0.036	0.072±0.033
	β	0.966±0.167	0.751±0.092	1.207±0.226	0.949±0.196
	γ	1.229±0.338	1.545±0.311	1.367±0.374	1.405±0.378
	A_a	1.713±0.327	2.347±0.971	2.189±0.964	2.245±0.936
	A_f	1.340±0.232	1.305±0.211	1.315±0.269	1.319±0.284
	r^2	0.978	0.978	0.979	0.983
	p	0.722	0.801	0.788	0.957
Behavioral and N1P1-neuronal	N_a	0.039±0.019	0.053±0.037	0.016±0.001	0.037±0.022
	N_m	0.070±0.029	0.135±0.158	0.063±0.029	0.068±0.029
	β	1.934±0.094	2.145±0.281	1.926±0.066	1.979±0.144
	γ	1.401±0.260	1.593±0.476	1.926±0.302	1.574±0.351
	A	0.385±0.034	0.332±0.052	0.304±0.017	0.337±0.031
	A_a	1.774±0.410	1.501±0.377	1.739±0.376	1.664±0.406
	A_f	1.300±0.144	1.188±0.159	1.239±0.111	1.238±0.142
	r^2	0.980	0.972	0.991	0.991
	p	1.000	1.000	1.000	1.000

Note: N_a, standard deviation of additive internal noise; N_m, standard deviation of multiplicative internal noise; β, gain from template matching; γ, nonlinearity exponent; A, parameter for normalization of template gain between psychophysical and neuronal performance; A_a, parameter associated with signal enhancement equivalent to internal additive noise reduction; A_f, parameter associated with external noise exclusion; r^2, goodness of fit; p indicates p value of f-test between reduced model (A_a & A_f) and most saturated model.

Because of a similar top-down effect on behavioral and N1P1-neuronal TvCs, the behavioral and N1P1-neuronal TvC functions were also fitted together with PTM.

functions ($r^2 > 0.97$) consisted of a mixture of two mechanisms (Table 1): increased internal additive noise (as indicated by an A_a of 1.664 ± 0.406) and increased impact of external noise (as indicated by an A_f of 1.238 ± 0.142). This model was statistically equivalent to the most saturated model with three mechanisms (all $p = 1.0$, Table 1) and was superior to all its reduced models (all $p < 0.05$, Table 2).

Table 2. P vaules of the nested model tests of the reduced models (No change, A_a, A_m, A_f, A_a & A_m, A_a, & A_f, and A_m & A_f) and the most saturated model in each cat (Cat1, Cat2, and Cat3) and their average (Cat1–3) before and after top-down influence was suppressed by c-tDCS in A7

TvC functions	Fitting model	Cat1	Cat2	Cat3	Cat1-3
Behavioral	No change	0.0002	<0.0001	<0.0001	<0.0001
	A_a	0.0229	0.0427	0.0231	0.0363
	A_m	0.0015	0.0014	0.0008	0.0009
	A_f	0.0016	0.0002	0.0001	0.0001
	A_a & A_m	0.0067	0.0354	0.0228	0.0326
	A_a & A_f	0.9993	0.5596	1.0000	1.0000
	A_m & A_f	0.0004	0.0004	0.0002	0.0003
N1P1-neuronal	No change	<0.0001	<0.0001	<0.0001	<0.0001
	A_a	0.0446	0.0461	0.0154	0.0133
	A_m	0.0009	0.0002	0.0001	<0.0001
	A_f	0.0003	<0.0001	<0.0001	<0.0001
	A_a & A_m	0.0129	0.0149	0.0053	0.0139
	A_a & A_f	0.8197	0.9981	1.0000	0.4385
	A_m & A_f	<0.0001	<0.0001	<0.0001	<0.0001
P1N2-neuronal	No change	<0.0001	0.0002	<0.0001	<0.0001
	A_a	0.0445	0.0380	0.0447	0.0258
	A_m	<0.0001	0.0010	<0.0001	<0.0001
	A_f	0.0002	0.0008	<0.0001	<0.0001
	A_a & A_m	0.0198	0.0273	0.0144	0.0070
	A_a & A_f	0.7215	0.8012	0.7884	0.9569
	A_m & A_f	<0.0001	0.0002	<0.0001	<0.0001
Behavioral and N1P1-neuronal	No change	<0.0001	0.0128	<0.0001	<0.0001
	A_a	0.0234	0.0495	0.0065	0.0132
	A_m	0.0008	0.0205	0.0007	0.0005
	A_f	0.0003	0.0220	0.0002	0.0001
	A_a & A_m	0.0087	0.0243	0.0060	0.0111
	A_a & A_f	1.0000	1.0000	1.0000	1.0000
	A_m & A_f	0.0004	0.0428	0.0004	0.0002

Note: A_a, parameter associated with signal enhancement or equivalent to internal additive noise reduction; A_m, parameter associated with the proportional constant of multiplicative noise; A_f, parameter associated with external noise exclusion.

The PTM analysis suggested that suppressing top-down influence of A7 decreased behavioral and neuronal contrast sensitivity through a combined mechanism of increased internal additive noise and increased impact of external noise.

DISCUSSION

In this study, we examined top-down influence of area 7 (A7), a high-level visual cortical area of cat (Han et al., 2008; Olson and Lawler, 1987; Yang et al., 2016b), on behavioral and V1 neuronal contrast sensitivity function (CSF) and contrast threshold versus external noise contrast (TvC) function. The top-down influence of A7 was modulated using tDCS, a noninvasive tool that could reversibly regulate neuronal activity in the stimulated local brain region (Impey et al., 2016; Krause et al., 2013; Kunori and Takashima, 2019; Pan et al., 2021a). Behavioral CSF and TvC functions were measured using the staircase method (Dosher and Lu, 1999, 2005; Hua et al., 2010; Lu and Dosher, 1998; Meng et al., 2013; Zhou et al., 2006). Neuronal CSF and TvC functions in V1 was assessed by visual evoked potentials (VEP), which reflect membrane potentials from a large population of neurons at a high temporal resolution (Haider et al., 2016; Si et al., 2016; Tokashiki

et al., 2018; Tomiyama et al., 2016; Whittingstall et al., 2008). We found that suppressing top-down influence of A7 with cathode (c)-tDCS, but not sham (s)-tDCS, significantly reduced both behavioral and V1 neuronal contrast sensitivity in the same range of spatial frequencies (SFs) and significantly increased both behavioral and neuronal contrast thresholds over the same range of external noise levels. The neuronal CSFs and TvC functions were highly correlated with their behavioral counterparts both before and after suppression of the top-down influence. Analysis of the TvC functions with the Perceptual Template Model (Dosher and Lu, 1999; Huang et al., 2008, 2009; Lu et al., 2005; Lu and Dosher, 2008) showed that suppression of top-down influence increased internal additive noise and the impact of external noise at both the behavioral and neuronal levels. These results indicate that top-down influence of A7 increases behavioral and V1 neuronal contrast sensitivity through reducing internal additive noise and the impact of external noise.

Top-down influence of A7 on V1 neuronal activity

In this study, we first confirmed the top-down influence of A7 on V1 neuronal activity by examining VEP changes in V1 before and after tDCS in A7. We found that c-tDCS of A7 significantly reduced VEP amplitudes but not latencies in V1, whereas s-tDCS of A7 and c-tDCS in the adjacent nonvisual cortical area A5 had no significant impact. Furthermore, our previous studies have shown that neuronal response in V1 was not significantly affected by c-tDCS of higher-order visual cortical areas A7 and 21a after neuronal activity in those areas was abolished by electrolytic lesions (Ding et al., 2021; Pan et al., 2021a). These results demonstrated that c-tDCS of A7 suppressed neuronal activity in V1 through a reduction of top-down influence from A7, not through diffusion of electrical current across cortical areas.

Our results suggest that the normal top-down influence of A7 in the absence of c-tDCS enhances neuronal activity in V1, consistent with previous studies in neuroimaging (Chen et al., 2014; Galuske et al., 2002; Huang et al., 2004; Liang et al., 2007; Tong et al., 2011; Yang et al., 2016b) and single-unit recordings (Huh et al., 2018; Jansen-Amorim et al., 2012; Wang et al., 2000, 2007, 2010; Zhang et al., 2014). Our results are also supported by neuronal tracing studies that showed that most feedback neurons are CaMKII-positive pyramidal neurons (Budd, 1998; Han et al., 2008; Johnson and Burkhalter, 1994, 1997; Pan et al., 2021b) and may use primarily excitatory amino acid as neurotransmitters (Johnson and Burkhalter, 1994; van Loon et al., 2015). The observed excitatory top-down influence of A7 on V1 is, however, different from reports of inhibitory top-down effects of V2/V3 on V1 neurons in primate and rodent studies (Hishida et al., 2019; Maniglia et al., 2019; Nassi et al., 2013, 2014). The different effects of top-down influence suggest that the type of top-down influence may depend on the specific higher-level cortical area or neuronal circuitry in different animal species. For example, feedback from the mouse frontal cortex has been shown to activate inhibitory neurons through local circuitry in V1 (Zhang et al., 2014); this may explain why some authors report a bidirectional top-down influence of enhancement and suppression on V1 neurons (Cox et al., 2019; Klink et al., 2017; Nurminen et al., 2018). Further studies are necessary to clarify these different observations.

Top-down influence of A7 on behavioral and V1 neuronal contrast sensitivity

How visual signals are processed by the visual system is under debate for decades (Crick and Koch, 1995; Kang and Maunsell, 2020; Liu et al., 2020; Murphey and Maunsell, 2007; Riesenhuber and Poggio, 1999). Based on the neuronal receptive field properties along the visual pathway (Hubel and Wiesel, 1968; van Kleef et al., 2010), it is generally thought that visual perception is formed through feedforward processing in which information flows from low-level visual cortical areas to high-level cortical areas (Crick and Koch, 1995; Riesenhuber and Poggio, 1999; Serre et al., 2007). Because top-down influence can affect visual detection (Ahissar and Hochstein, 2000; Dosher and Lu, 2000a; Hupé et al., 1998; Ro et al., 2003) and neuronal activity in V1 (Galuske et al., 2002; Lee, 2002; Pascual-Leone and Walsh, 2001; Wang et al., 2000), some have proposed that visual perception may occur in a reverse hierarchy with both feedforward and feedback processing loops mediated by recurrent connections between V1 and higher-order cortical areas (Juan et al., 2004; Juan and Walsh, 2003). However, the relative contributions of top-down feedback and V1 remain elusive. Some studies have emphasized the role of top-down influence (Al-Aidroos et al., 2012; Chalk et al., 2010; Eger et al., 2007; Fenske et al., 2006; Gazzaley et al., 2005; Gilbert and Li, 2013; Huang and Dobkins, 2005; Kamiyama et al., 2016; Keller et al., 2020; Lee and Maunsell, 2010; Li et al., 2008; Manita et al., 2015; Nassi et al., 2013; Nurminen et al., 2018; Pak et al., 2020; Roland et al., 2006; Rolls, 2008; Wang et al., 2013; Zhang et al., 2014). Other studies have showed that V1, including back projections to V1, is crucial for visual detection (Chirimuuta and Tolhurst, 2005; Gerard-Mercier et al., 2016; Glickfeld et al., 2013; Hurme et al., 2017, 2019; Koivisto et al., 2010; Roebuck et al., 2014; Seidemann and Geisler, 2018; Silvanto et al.,

2005a, 2005b). Furthermore, the necessity of V1 for conscious visual perception is strongly supported by the blindsight phenomenon (Cowey, 2010; Stoerig and Cowey, 1995, 2007). However, recent studies report that patients without V1 can perceive phosphenes in their blind hemifields when transcranial magnetic stimulation is applied over the ipsilesional parietal cortical region (Mazzi et al., 2014), suggesting that visual perception can occur without any contribution from V1 (Mazzi et al., 2019; Silvanto, 2014, 2015), and thus may challenge the reverse hierarchy model and the necessity of V1 in visual perception.

The brain mechanism of contrast detection, which is fundamental to the perception of object shape, size, and motion features (Baker, 2013; Ginsburg, 2006), is also in debate. Numerous studies have highlighted the role of V1 in contrast detection because of the relationship between V1 neuronal contrast-response functions and behavioral contrast detection performance (Albrecht, 1995; Anzai et al., 1995; Chirimuuta and Tolhurst, 2005; Clatworthy et al., 2003), especially the well-predicted behavioral contrast detection performance from pooled neuronal responses to stimulus contrasts in V1 or other early visual cortical areas (Busse et al., 2011; Chirimuuta and Tolhurst, 2005; Glickfeld et al., 2013; Niemeyer and Paradiso, 2016; Parisi et al., 2006; Ress and Heeger, 2003). Our previous studies showed that the behavioral CSF measured in cat was highly correlated with the neuronal CSF constructed from neuronal responses in V1 (Meng et al., 2013), and perceptual learning of contrast detection improved both behavioral and V1 neuronal CSFs around the trained spatial frequency (Hua et al., 2010). Conversely, other studies have shown that top-down influence can also modulate behavioral contrast sensitivity (Cutrone et al., 2014; Dosher and Lu, 2000a; Han and VanRullen, 2016; Lu and Dosher, 1998). Still others report that top-down influence may affect neuronal contrast sensitivity in V1 or low-level visual cortex (Li et al., 2008; Maniglia et al., 2019; Nauhaus et al., 2009; Thiele et al., 2009; Williford and Maunsell, 2006; Zhang et al., 2014). All these results led to the hypothesis that top-down influence from higher-order cortex may affect contrast detection through modulation of neuronal contrast sensitivity in V1.

The current study examined the hypothesis by investigating the dual effects of top-down influence of high-level visual cortex on behavioral and V1 neuronal contrast sensitivity in cat. We found that suppressing top-down influence of A7 concurrently reduced behavioral and neuronal contrast sensitivity in the same spatial frequency range. In addition, the behavioral and V1 neuronal contrast sensitivity functions were highly correlated with each other both before and after the top-down influence suppression, suggesting that top-down influence may affect behavioral contrast detection by modifying neuronal contrast sensitivity in V1. Specifically, the neuronal contrast sensitivity measured by the early VEP components (N1P1) was equally affected by top-down suppression as the behavioral contrast sensitivity, whereas the neuronal contrast sensitivity measured by the later VEP components (P1N2) was more affected by top-down suppression than the behavioral contrast sensitivity. The results suggest that top-down influence of A7 affects both early and later responses in V1, consistent with some previous studies (Foster et al., 2021; Kelly and Mohr, 2018; Zhang et al., 2015), but inconsistent with other studies that report top-down effects only on the later responses in V1 (Alilović et al., 2019; Baumgartner et al., 2018; Kirchberger et al., 2021). Future studies are necessary to clarify if top-down effects on the early and late response components in V1 depend on the strength of the top-down influence in different tasks (Kelly and Mohr, 2018; Slotnick, 2018) or the source of top-down influence (Johnson and Burkhalter, 1997; Pan et al., 2021b). We found that behavioral contrast detection is more highly coupled to early sensory responses in V1, which is consistent with previous observations (Bao et al., 2010; Richter et al., 2018; Zhang et al., 2015). Furthermore, our modeling analysis indicated that suppressing top-down influence of A7 affected behavioral and neuronal contrast sensitivity through a mixture mechanism of increased internal additive noise and increased impact of external noise, providing the first evidence that top-down influence may modulate behavioral contrast detection through regulation of neuronal contrast sensitivity in V1. The results provide an evidence that challenges the feedforward hierarchical visual processing model and supports the reverse hierarchy theory about visual perception based on information processing loops mediated by recurrent connections between V1 and higher-level cortical areas (Johnson and Burkhalter, 1997; Juan et al., 2004; Juan and Walsh, 2003; Koivisto et al., 2010; Tong, 2003).

Limitations of the study

In this study, we found that suppression of top-down influence from A7 had similar effects on behavioral and V1 neuronal contrast sensitivity. There are several limitations that need to be addressed in future investigations.

First, the current study used tDCS to modulate top-down influence from A7. Although tDCS is a noninvasive tool and can reversibly modulate neuronal activity in a local brain area (Impey et al., 2016; Kunori and

Takashima, 2019; Nitsche and Paulus, 2000; Pan et al., 2021a; Zhao et al., 2020), it is unknown if the results observed in this study can be generalized to studies using different manipulation methods, such as GABA/GABA receptor's agonists application (Chen et al., 2014; Hishida et al., 2019; Tong et al., 2011), cortical cooling (Bardy et al., 2009; Nassi et al., 2013; Wang et al., 2000), optogenetic manipulation (Huh et al., 2018; Kirchberger et al., 2021; Zhang et al., 2014), and attention control (Al-Aidroos et al., 2012; Baumgartner et al., 2018; Gilbert and Sigman, 2007; Li et al., 2008). We are working on new experiments to test the generalizability of the results observed in this study.

Second, this study assessed neuronal contrast sensitivity using VEP from V1. Although VEP provides a measure of activities from large populations of neurons (Haider et al., 2016; Tokashiki et al., 2018; Whittingstall et al., 2008) and exhibits tuning responses for stimulus orientation, motion direction, contrast and size similar to single- or multi-unit responses (Kayser and König, 2004; Lashgari et al., 2012), it contains a wide range of frequency components that may have different relationships with single/multi-unit responses (Lashgari et al., 2012) and visual perception (Gail et al., 2004; Han et al., 2021; Henrie and Shapley, 2005; Richter et al., 2018; Wang et al., 2016). Subsequent studies need to further examine top-down influence on V1 neuronal contrast sensitivity using simultaneous recordings and analysis of unit response and local field potentials.

Finally, considering that top-down effects may be considerably reduced under anesthesia (Keller et al., 2020), future studies should conduct electrophysiological recording in awake cats using microelectrode-array implantation and optogenetic modulation techniques (Huh et al., 2018; Kirchberger et al., 2021; Zhang et al., 2014).

STAR★METHODS

Detailed methods are provided in the online version of this paper and include the following:

- KEY RESOURCES TABLE
- RESOURCE AVAILABILITY
  - Lead contact
  - Materials availability
  - Data and code availability
- EXPERIMENTAL MODEL AND SUBJECT DETAILS
- METHOD DETAILS
  - Preparation for VEP recording in V1 cortex
  - Administration of transcranial direct current stimulation
  - Psychophysical measurement of behavioral contrast sensitivity
  - VEP recording and visual stimuli
- QUANTIFICATION AND STATISTICAL ANALYSIS
  - Evaluation of top-down influence on neuronal activity in V1
  - Construct neuronal CSF and TvC functions with ROC analysis
  - Comparisons of behavioral and neuronal CSF and TvC functions
  - PTM modeling analysis

SUPPLEMENTAL INFORMATION

Supplemental information can be found online at https://doi.org/10.1016/j.isci.2021.103683

ACKNOWLEDGMENTS

This work was supported by grants from the National Natural Science Foundation of China (31771181), Anhui Provincial Key Laboratory of the Conservation and Exploitation of Biological Resources (591601), Anhui Provincial Key Laboratory of Molecular Enzymology and Mechanism of Major Diseases, and Key Laboratory of Biomedicine in Gene Diseases and Health of Anhui Higher Education Institutes.

AUTHOR CONTRIBUTIONS

JD, ZY, TH, and ZL: study design; JD, ZY, XH, and QS: cat behavioral training and psychophysical measurement of CSF and TvC functions; JD, ZY, HY, FX, SZ, YT, and QZ: surgery and electrophysiological recording of VEPs in V1; JD, ZY, HY, FX, XH, SZ, YT, QZ, and QS: psychophysical and neuronal data analysis. All

authors have made contributions to data interpretation, manuscript drafting, and revising and have approved the final version of the manuscript.

DECLARATION OF INTERESTS

All affiliations are listed on the title page of the manuscript. All funding sources for this study are listed in the "Acknowledgments" section of the manuscript. We, the authors and our immediate family members have no financial interests to declare. We, the authors and our immediate family members, have no positions to declare and are not members of the journal's advisory board. The authors and our immediate family members have no related patents to declare. The authors declare no competing interests.

Received: July 27, 2021
Revised: November 16, 2021
Accepted: December 20, 2021
Published: January 21, 2022

REFERENCES

Adab, H.Z., and Vogels, R. (2011). Practicing coarse orientation discrimination improves orientation signals in macaque cortical area v4. Curr. Biol. *21*, 1661–1666.

Ahissar, M., and Hochstein, S. (2000). The spread of attention and learning in feature search: effects of target distribution and task difficulty. Vis. Res *40*, 1349–1364. https://doi.org/10.1016/s0042-6989(00)00002-x.

Al-Aidroos, N., Said, C.P., and Turk-Browne, N.B. (2012). Top-down attention switches coupling between low-level and high-level areas of human visual cortex. Proc. Natl. Acad. Sci. U S A *109*, 14675–14680. https://doi.org/10.1073/pnas.1202095109.

Albrecht, D.G. (1995). Visual cortex neurons in monkey and cat: effect of contrast on the spatial and temporal phase transfer functions. Vis. Neurosci. *12*, 1191–1210.

Alilović, J., Timmermans, B., Reteig, L.C., van Gaal, S., and Slagter, H.A. (2019). No evidence that predictions and attention modulate the first feedforward sweep of cortical information processing. Cerebral Cortex *29*, 2261–2278. https://doi.org/10.1093/cercor/bhz038.

Angelucci, A., Bijanzadeh, M., Nurminen, L., Federer, F., Merlin, S., and Bressloff, P.C. (2017). Circuits and mechanisms for surround modulation in visual cortex. Annu. Rev. Neurosci. *40*, 425–451. https://doi.org/10.1146/annurev-neuro-072116-031418.

Angelucci, A., and Bressloff, P.C. (2006). Contribution of feedforward, lateral and feedback connections to the classical receptive field center and extra-classical receptive field surround of primate V1 neurons. Prog. Brain Res. *154*, 93–120. https://doi.org/10.1016/s0079-6123(06)54005-1.

Anzai, A., Bearse, M.A., Jr., Freeman, R.D., and Cai, D. (1995). Contrast coding by cells in the cat's striate cortex: monocular vs. binocular detection. Vis. Neurosci. *12*, 77–93.

Avendaño, C., Rausell, E., Perez-Aguilar, D., and Isorna, S. (1988). Organization of the association cortical afferent connections of area 5: a retrograde tracer study in the cat. J. Comp. Neurol. *278*, 1–33. https://doi.org/10.1002/cne.902780102.

Aydin-Abidin, S., Moliadze, V., Eysel, U.T., and Funke, K. (2006). Effects of repetitive TMS on visually evoked potentials and EEG in the anaesthetized cat: dependence on stimulus frequency and train duration. J. Physiol. *574*, 443–455. https://doi.org/10.1113/jphysiol.2006.108464.

Bachtiar, V., Near, J., Johansen-Berg, H., and Stagg, C.J. (2015). Modulation of GABA and resting state functional connectivity by transcranial direct current stimulation. eLife *4*, e08789. https://doi.org/10.7554/eLife.08789.

Baker, D.H. (2013). What is the primary cause of individual differences in contrast sensitivity? PLoS One *8*, e69536. https://doi.org/10.1371/journal.pone.0069536.

Bao, M., Yang, L., Rios, C., He, B., and Engel, S.A. (2010). Perceptual learning increases the strength of the earliest signals in visual cortex. J. Neurosci. *30*, 15080–15084.

Bardy, C., Huang, J.Y., Wang, C., Fitzgibbon, T., and Dreher, B. (2009). Top-down' influences of ipsilateral or contralateral postero-temporal visual cortices on the extra-classical receptive fields of neurons in cat's striate cortex. Neuroscience *158*, 951–968. https://doi.org/10.1016/j.neuroscience.2008.09.057.

Barlow, H.B., Kaushal, T.P., Hawken, M., and Parker, A.J. (1987). Human contrast discrimination and the threshold of cortical neurons. J. Opt. Soc. Am. A *4*, 2366–2371.

Baumgartner, H.M., Graulty, C.J., Hillyard, S.A., and Pitts, M.A. (2018). Does spatial attention modulate the earliest component of the visual evoked potential? Cogn. Neurosci. *9*, 4–19. https://doi.org/10.1080/17588928.2017.1333490.

Brainard, D.H. (1997). The psychophysics toolbox. Spat. Vis. *10*, 433–436.

Budd, J.M. (1998). Extrastriate feedback to primary visual cortex in primates: a quantitative analysis of connectivity. Proc. Biol. Sci. *265*, 1037–1044. https://doi.org/10.1098/rspb.1998.0396.

Busse, L., Ayaz, A., Dhruv, N.T., Katzner, S., Saleem, A.B., Schölvinck, M.L., Zaharia, A.D., and Carandini, M. (2011). The detection of visual contrast in the behaving mouse. J. Neurosci. *31*, 11351.

Chalk, M., Herrero, J.L., Gieselmann, M.A., Delicato, L.S., Gotthardt, S., and Thiele, A. (2010). Attention reduces stimulus-driven gamma frequency oscillations and spike field coherence in V1. Neuron *66*, 114–125. https://doi.org/10.1016/j.neuron.2010.03.013.

Chen, Y., Li, H., Jin, Z., Shou, T., and Yu, H. (2014). Feedback of the amygdala globally modulates visual response of primary visual cortex in the cat. NeuroImage *84*, 775–785. https://doi.org/10.1016/j.neuroimage.2013.09.010.

Chirimuuta, M., and Tolhurst, D.J. (2005). Does a Bayesian model of V1 contrast coding offer a neurophysiological account of human contrast discrimination? Vis. Res *45*, 2943–2959. https://doi.org/10.1016/j.visres.2005.06.022.

Clatworthy, P.L., Chirimuuta, M., Lauritzen, J.S., and Tolhurst, D.J. (2003). Coding of the contrasts in natural images by populations of neurons in primary visual cortex (V1). Vis. Res *43*, 1983–2001.

Connolly, J.D., Hashemi-Nezhad, M., and Lyon, D.C. (2012). Parallel feedback pathways in visual cortex of cats revealed through a modified rabies virus. J. Comp. Neurol. *520*, 988–1004. https://doi.org/10.1002/cne.22748.

Cowey, A. (2010). The blindsight saga. Exp. Brain Res. *200*, 3–24. https://doi.org/10.1007/s00221-009-1914-2.

Cox, M.A., Dougherty, K., Adams, G.K., Reavis, E.A., Westerberg, J.A., Moore, B.S., Leopold, D.A., and Maier, A. (2019). Spiking suppression precedes cued attentional enhancement of neural responses in primary visual Cortex. Cerebral Cortex *29*, 77–90. https://doi.org/10.1093/cercor/bhx305.

Crick, F., and Koch, C. (1995). Are we aware of neural activity in primary visual cortex? Nature *375*, 121–123. https://doi.org/10.1038/375121a0.

Cutrone, E.K., Heeger, D.J., and Carrasco, M. (2014). Attention enhances contrast appearance

via increased input baseline of neural responses. J. Vis. *14*, 16. https://doi.org/10.1167/14.14.16.

De Weerd, P., Vandenbussche, E., and Orban, G.A. (1990). Bar orientation discrimination in the cat. Vis. Neurosci. *4*, 257–268.

Ding, J., Hu, X., Xu, F., Yu, H., Ye, Z., Zhang, S., Pan, H., Pan, D., Tu, Y., Zhang, Q., et al. (2021). Suppression of top-down influence decreases neuronal excitability and contrast sensitivity in the V1 cortex of cat. Sci. Rep. *11*, 16034. https://doi.org/10.1038/s41598-021-95407-7.

Ding, Z., Li, J., Spiegel, D.P., Chen, Z., Chan, L., Luo, G., Yuan, J., Deng, D., Yu, M., and Thompson, B. (2016). The effect of transcranial direct current stimulation on contrast sensitivity and visual evoked potential amplitude in adults with amblyopia. Sci. Rep. *6*, 19280. https://doi.org/10.1038/srep19280.

Dosher, B.A., Jeter, P., Liu, J., and Lu, Z.L. (2013). An integrated reweighting theory of perceptual learning. Proc. Natl. Acad. Sci. U S A *110*, 13678–13683. https://doi.org/10.1073/pnas.1312552110.

Dosher, B.A., and Lu, Z.-L. (2005). Perceptual learning in clear displays optimizes perceptual expertise: learning the limiting process. Proc. Natl. Acad. Sci. U S A *102*, 5286–5290.

Dosher, B.A., and Lu, Z.L. (1999). Mechanisms of perceptual learning. Vis. Res *39*, 3197–3221.

Dosher, B.A., and Lu, Z.L. (2000a). Mechanisms of perceptual attention in precuing of location. Vis. Res *40*, 1269–1292.

Dosher, B.A., and Lu, Z.L. (2000b). Noise exclusion in spatial attention. Psychol. Sci. *11*, 139–146.

Dreher, B., Wang, C., Turlejski, K.J., Djavadian, R.L., and Burke, W. (1996). Areas PMLS and 21a of cat visual cortex: two functionally distinct areas. Cereb. Cortex *6*, 585–599.

Edwards, D.P., Purpura, K.P., and Kaplan, E. (1995). Contrast sensitivity and spatial frequency response of primate cortical neurons in and around the cytochrome oxidase blobs. Vis. Res *35*, 1501–1523.

Eger, E., Henson, R.N., Driver, J., and Dolan, R.J. (2007). Mechanisms of top-down facilitation in perception of visual objects studied by FMRI. Cerebral cortex *17*, 2123–2133. https://doi.org/10.1093/cercor/bhl119.

Federer, F., Ta'afua, S., Merlin, S., Hassanpour, M.S., and Angelucci, A. (2021). Stream-specific feedback inputs to the primate primary visual cortex. Nat. Commun. *12*, 228. https://doi.org/10.1038/s41467-020-20505-5.

Fenske, M.J., Aminoff, E., Gronau, N., and Bar, M. (2006). Top-down facilitation of visual object recognition: object-based and context-based contributions. Prog. Brain Res. *155*, 3–21. https://doi.org/10.1016/s0079-6123(06)55001-0.

Foster, J.J., Thyer, W., Wennberg, J.W., and Awh, E. (2021). Covert attention increases the gain of stimulus-evoked population codes. J. Neurosci. *41*, 1802–1815. https://doi.org/10.1523/jneurosci.2186-20.2020.

Gail, A., Brinksmeyer, H.J., and Eckhorn, R. (2004). Perception-related modulations of local field potential power and coherence in primary visual cortex of awake monkey during binocular rivalry. Cerebral Cortex *14*, 300–313. https://doi.org/10.1093/cercor/bhg129.

Galuske, R.A., Schmidt, K.E., Goebel, R., Lomber, S.G., and Payne, B.R. (2002). The role of feedback in shaping neural representations in cat visual cortex. Proc. Natl. Acad. Sci. U S A *99*, 17083–17088. https://doi.org/10.1073/pnas.242399199.

Gazzaley, A., Cooney, J.W., McEvoy, K., Knight, R.T., and D'Esposito, M. (2005). Top-down enhancement and suppression of the magnitude and speed of neural activity. J. Cogn. Neurosci. *17*, 507–517. https://doi.org/10.1162/0898929053279522.

Geisler, W.S., and Albrecht, D.G. (1997). Visual cortex neurons in monkeys and cats: detection, discrimination, and identification. Vis. Neurosci. *14*, 897–919. https://doi.org/10.1017/s0952523800011627.

Gerard-Mercier, F., Carelli, P.V., Pananceau, M., Troncoso, X.G., and Frégnac, Y. (2016). Synaptic correlates of low-level perception in V1. J. Neurosci. *36*, 3925–3942. https://doi.org/10.1523/jneurosci.4492-15.2016.

Gilbert, C.D., and Li, W. (2013). Top-down influences on visual processing. Nat. Rev. Neurosci. *14*, 350–363. https://doi.org/10.1038/nrn3476.

Gilbert, C.D., and Sigman, M. (2007). Brain states: top-down influences in sensory processing. Neuron *54*, 677–696.

Ginsburg, A.P. (2006). Contrast sensitivity: determining the visual quality and function of cataract, intraocular lenses and refractive surgery. Curr. Opin. Ophthalmol. *17*, 19–26.

Glickfeld, L.L., Histed, M.H., and Maunsell, J.H. (2013). Mouse primary visual cortex is used to detect both orientation and contrast changes. J. Neurosci. *33*, 19416–19422. https://doi.org/10.1523/jneurosci.3560-13.2013.

Haider, B., Schulz, D.P., Hausser, M., and Carandini, M. (2016). Millisecond coupling of local field potentials to synaptic currents in the awake visual cortex. Neuron *90*, 35–42. https://doi.org/10.1016/j.neuron.2016.02.034.

Han, B., and VanRullen, R. (2016). Shape perception enhances perceived contrast: evidence for excitatory predictive feedback? Scientific Rep. *6*, 22944. https://doi.org/10.1038/srep22944.

Han, C., Wang, T., Wu, Y., Li, Y., Yang, Y., Li, L., Wang, Y., and Xing, D. (2021). The generation and modulation of distinct gamma oscillations with local, horizontal, and feedback connections in the primary visual cortex: a model study on large-scale networks. Neural Plasticity *2021*, 8874516. https://doi.org/10.1155/2021/8874516.

Han, Y., Yang, X., Chen, Y., and Shou, T. (2008). Evidence for corticocortical connections between areas 7 and 17 in cerebral cortex of the cat. Neurosci. Lett. *430*, 70–74. https://doi.org/10.1016/j.neulet.2007.10.022.

Harrison, L.M., Stephan, K.E., Rees, G., and Friston, K.J. (2007). Extra-classical receptive field effects measured in striate cortex with fMRI. NeuroImage *34*, 1199–1208. https://doi.org/10.1016/j.neuroimage.2006.10.017.

Henrie, J.A., and Shapley, R. (2005). LFP power spectra in V1 cortex: the graded effect of stimulus contrast. J. Neurophysiol. *94*, 479–490. https://doi.org/10.1152/jn.00919.2004.

Hicks, T.P., Benedek, G., and Thurlow, G.A. (1988). Modality specificity of neuronal responses within the cat's insula. J. Neurophysiol. *60*, 422–437. https://doi.org/10.1152/jn.1988.60.2.422.

Hishida, R., Horie, M., Tsukano, H., Tohmi, M., Yoshitake, K., Meguro, R., Takebayashi, H., Yanagawa, Y., and Shibuki, K. (2019). Feedback inhibition derived from the posterior parietal cortex regulates the neural properties of the mouse visual cortex. Eur. J. Neurosci. *50*, 2970–2987. https://doi.org/10.1111/ejn.14424.

Hood, D.C., Ghadiali, Q., Zhang, J.C., Graham, N.V., Wolfson, S.S., and Zhang, X. (2006). Contrast-response functions for multifocal visual evoked potentials: a test of a model relating V1 activity to multifocal visual evoked potentials activity. J. Vis. *6*, 580–593. https://doi.org/10.1167/6.5.4.

Hua, T., Bao, P., Huang, C.B., Wang, Z., Xu, J., Zhou, Y., and Lu, Z.L. (2010). Perceptual learning improves contrast sensitivity of V1 neurons in cats. Curr. Biol. *20*, 887–894.

Hua, T., Li, X., He, L., Zhou, Y., Wang, Y., and Leventhal, A.G. (2006). Functional degradation of visual cortical cells in old cats. Neurobiol. Aging *27*, 155–162.

Huang, C.B., Lu, Z.L., and Dosher, B.A. (2008). Co-learning analysis of two perceptual learning tasks with identical input stimuli supports the reweighting hypothesis. Vis. Res *8*, 1123.

Huang, C.B., Lu, Z.L., and Zhou, Y. (2009). Mechanisms underlying perceptual learning of contrast detection in adults with anisometropic amblyopia. J. Vis. *9*, 24 21–14.

Huang, J.Y., Wang, C., and Dreher, B. (2017). Silencing "Top-Down" cortical signals affects spike-responses of neurons in cat's "intermediate" visual cortex. Front. Neural circuits *11*, 27. https://doi.org/10.3389/fncir.2017.00027.

Huang, L., Chen, X., and Shou, T. (2004). Spatial frequency-dependent feedback of visual cortical area 21a modulating functional orientation column maps in areas 17 and 18 of the cat. Brain Res. *998*, 194–201.

Huang, L., and Dobkins, K.R. (2005). Attentional effects on contrast discrimination in humans: evidence for both contrast gain and response gain. Vis. Res. *45*, 1201–1212. https://doi.org/10.1016/j.visres.2004.10.024.

Hubel, D.H., and Wiesel, T.N. (1968). Receptive fields and functional architecture of monkey striate cortex. J. Physiol. *195*, 215–243.

Huh, C.Y.L., Peach, J.P., Bennett, C., Vega, R.M., and Hestrin, S. (2018). Feature-specific organization of feedback pathways in mouse

visual cortex. Curr. Biol. *28*, 114–120.e115. https://doi.org/10.1016/j.cub.2017.11.056.

Hupé, J.M., James, A.C., Payne, B.R., Lomber, S.G., Girard, P., and Bullier, J. (1998). Cortical feedback improves discrimination between figure and background by V1, V2 and V3 neurons. Nature *394*, 784–787. https://doi.org/10.1038/29537.

Hurme, M., Koivisto, M., Revonsuo, A., and Railo, H. (2017). Early processing in primary visual cortex is necessary for conscious and unconscious vision while late processing is necessary only for conscious vision in neurologically healthy humans. NeuroImage *150*, 230–238. https://doi.org/10.1016/j.neuroimage.2017.02.060.

Hurme, M., Koivisto, M., Revonsuo, A., and Railo, H. (2019). V1 activity during feedforward and early feedback processing is necessary for both conscious and unconscious motion perception. NeuroImage *185*, 313–321. https://doi.org/10.1016/j.neuroimage.2018.10.058.

Impey, D., de la Salle, S., and Knott, V. (2016). Assessment of anodal and cathodal transcranial direct current stimulation (tDCS) on MMN-indexed auditory sensory processing. Brain Cogn. *105*, 46–54. https://doi.org/10.1016/j.bandc.2016.03.006.

Jansen-Amorim, A.K., Fiorani, M., and Gattass, R. (2012). GABA inactivation of area V4 changes receptive-field properties of V2 neurons in Cebus monkeys. Exp. Neurol. *235*, 553–562. https://doi.org/10.1016/j.expneurol.2012.03.008.

Jeon, S.T., Maurer, D., and Lewis, T.L. (2014). Developmental mechanisms underlying improved contrast thresholds for discriminations of orientation signals embedded in noise. Front Psychol. *5*, 977. https://doi.org/10.3389/fpsyg.2014.00977.

Johnson, R.R., and Burkhalter, A. (1994). Evidence for excitatory amino acid neurotransmitters in forward and feedback corticocortical pathways within rat visual cortex. Eur. J. Neurosci. *6*, 272–286.

Johnson, R.R., and Burkhalter, A. (1997). A polysynaptic feedback circuit in rat visual cortex. J. Neurosci. *17*, 7129–7140.

Juan, C.H., Campana, G., and Walsh, V. (2004). Cortical interactions in vision and awareness: hierarchies in reverse. Prog. Brain Res. *144*, 117–130. https://doi.org/10.1016/s0079-6123(03)14408-1.

Juan, C.H., and Walsh, V. (2003). Feedback to V1: a reverse hierarchy in vision. Exp. Brain Res. *150*, 259–263. https://doi.org/10.1007/s00221-003-1478-5.

Kamiyama, A., Fujita, K., and Kashimori, Y. (2016). A neural mechanism of dynamic gating of task-relevant information by top-down influence in primary visual cortex. Bio Syst. *150*, 138–148. https://doi.org/10.1016/j.biosystems.2016.09.009.

Kang, I., and Maunsell, J.H.R. (2020). The correlation of neuronal signals with behavior at different levels of visual cortex and their relative reliability for behavioral decisions. J. Neurosci. *40*, 3751–3767. https://doi.org/10.1523/jneurosci.2587-19.2020.

Kayser, C., and König, P. (2004). Stimulus locking and feature selectivity prevail in complementary frequency ranges of V1 local field potentials. Eur. J. Neurosci. *19*, 485–489. https://doi.org/10.1111/j.0953-816x.2003.03122.x.

Keller, A.J., Roth, M.M., and Scanziani, M. (2020). Feedback generates a second receptive field in neurons of the visual cortex. Nature *582*, 545–549. https://doi.org/10.1038/s41586-020-2319-4.

Kelly, S.P., and Mohr, K.S. (2018). Task dependence of early attention modulation: the plot thickens. Cogn. Neurosci. *9*, 24–26. https://doi.org/10.1080/17588928.2017.1372407.

Kirchberger, L., Mukherjee, S., Schnabel, U.H., van Beest, E.H., Barsegyan, A., Levelt, C.N., Heimel, J.A., Lorteije, J.A.M., van der Togt, C., Self, M.W., and Roelfsema, P.R. (2021). The essential role of recurrent processing for figure-ground perception in mice. Sci. Adv. *7*. https://doi.org/10.1126/sciadv.abe1833.

Klink, P.C., Dagnino, B., Gariel-Mathis, M.A., and Roelfsema, P.R. (2017). Distinct feedforward and feedback effects of microstimulation in visual cortex reveal neural mechanisms of texture segregation. Neuron *95*, 209–220.e203. https://doi.org/10.1016/j.neuron.2017.05.033.

Koivisto, M., Mäntylä, T., and Silvanto, J. (2010). The role of early visual cortex (V1/V2) in conscious and unconscious visual perception. NeuroImage *51*, 828–834. https://doi.org/10.1016/j.neuroimage.2010.02.042.

Krause, B., Márquez-Ruiz, J., and Kadosh, R.C. (2013). The effect of transcranial direct current stimulation: a role for cortical excitation/inhibition balance? Front. Hum. Neurosci. *7*, 602. https://doi.org/10.3389/fnhum.2013.00602.

Kunori, N., and Takashima, I. (2019). Evaluation of acute anodal direct current stimulation-induced effects on somatosensory-evoked responses in the rat. Brain Res. *1720*, 146318. https://doi.org/10.1016/j.brainres.2019.146318.

Lajoie, K., Andujar, J.E., Pearson, K., and Drew, T. (2010). Neurons in area 5 of the posterior parietal cortex in the cat contribute to interlimb coordination during visually guided locomotion: a role in working memory. J. Neurophysiol. *103*, 2234–2254. https://doi.org/10.1152/jn.01100.2009.

Lashgari, R., Li, X., Chen, Y., Kremkow, J., Bereshpolova, Y., Swadlow, H.A., and Alonso, J.M. (2012). Response properties of local field potentials and neighboring single neurons in awake primary visual cortex. J. Neurosci. *32*, 11396–11413. https://doi.org/10.1523/jneurosci.0429-12.2012.

Lee, J., and Maunsell, J.H.R. (2010). The effect of attention on neuronal responses to high and low contrast stimuli. J. Neurophysiol. *104*, 960–971. https://doi.org/10.1152/jn.01019.2009.

Lee, T.S. (2002). Top-down influence in early visual processing: a Bayesian perspective. Physiol. Behav. *77*, 645–650.

Li, X., Lu, Z.L., Tjan, B.S., Dosher, B.A., and Chu, W. (2008). Blood oxygenation level-dependent contrast response functions identify mechanisms of covert attention in early visual areas. Proc. Natl. Acad. Sci. U S A *105*, 6202–6207.

Liang, Z., Shen, W., and Shou, T. (2007). Enhancement of oblique effect in the cat's primary visual cortex via orientation preference shifting induced by excitatory feedback from higher-order cortical area 21a. Neuroscience *145*, 377–383. https://doi.org/10.1016/j.neuroscience.2006.11.051.

Liu, Y., Li, M., Zhang, X., Lu, Y., Gong, H., Yin, J., Chen, Z., Qian, L., Yang, Y., Andolina, I.M., et al. (2020). Hierarchical representation for chromatic processing across macaque V1, V2, and V4. Neuron *108*, 538–550.e535. https://doi.org/10.1016/j.neuron.2020.07.037.

Lu, Z.-L., Chu, W., Dosher, B.A., and Lee, S. (2005). Independent perceptual learning in monocular and binocular motion systems. Proc. Natl. Acad. Sci. U S A *102*, 5624–5629.

Lu, Z.L., and Dosher, B.A. (1998). External noise distinguishes attention mechanisms. Vis. Res *38*, 1183–1198.

Lu, Z.L., and Dosher, B.A. (2004). Spatial attention excludes external noise without changing the spatial frequency tuning of the perceptual template. J. Vis. *4*, 955–966.

Lu, Z.L., and Dosher, B.A. (2008). Characterizing observers using external noise and observer models: assessing internal representations with external noise. Psychol. Rev. *115*, 44–82.

Lu, Z.L., Li, X., Tjan, B.S., Dosher, B.A., and Chu, W. (2011). Attention extracts signal in external noise: a BOLD fMRI study. J. Cogn. Neurosci. *23*, 1148–1159.

Maniglia, M., Trotter, Y., and Aedo-Jury, F. (2019). TMS reveals inhibitory extrastriate cortico-cortical feedback modulation of V1 activity in humans. Brain Struct. Funct. *224*, 3399–3408. https://doi.org/10.1007/s00429-019-01964-z.

Manita, S., Suzuki, T., Homma, C., Matsumoto, T., Odagawa, M., Yamada, K., Ota, K., Matsubara, C., Inutsuka, A., Sato, M., et al. (2015). A top-down cortical circuit for accurate sensory perception. Neuron *86*, 1304–1316. https://doi.org/10.1016/j.neuron.2015.05.006.

Mazzi, C., Mancini, F., and Savazzi, S. (2014). Can IPS reach visual awareness without V1? Evidence from TMS in healthy subjects and hemianopic patients. Neuropsychologia *64*, 134–144. https://doi.org/10.1016/j.neuropsychologia.2014.09.026.

Mazzi, C., Savazzi, S., and Silvanto, J. (2019). On the "blindness" of blindsight: what is the evidence for phenomenal awareness in the absence of primary visual cortex (V1)? Neuropsychologia *128*, 103–108. https://doi.org/10.1016/j.neuropsychologia.2017.10.029.

Meng, J., Liu, R., Wang, K., Hua, T., Lu, Z.L., and Xi, M. (2013). Neural correlates of stimulus spatial frequency-dependent contrast detection. Exp. Brain Res. *225*, 377–385.

Merrikhi, Y., Clark, K., and Noudoost, B. (2018). Concurrent influence of top-down and bottom-up inputs on correlated activity of Macaque extrastriate neurons. Nat. Commun. *9*, 5393. https://doi.org/10.1038/s41467-018-07816-4.

Monte-Silva, K., Kuo, M.-F., Liebetanz, D., Paulus, W., and Nitsche, M.A. (2010). Shaping the optimal repetition interval for cathodal transcranial direct

current stimulation (tDCS). J. Neurophysiol. *103*, 1735–1740. https://doi.org/10.1152/jn.00924.2009.

Murphey, D.K., and Maunsell, J.H. (2007). Behavioral detection of electrical microstimulation in different cortical visual areas. Curr. Biol. *17*, 862–867. https://doi.org/10.1016/j.cub.2007.03.066.

Murray, S.O., Kersten, D., Olshausen, B.A., Schrater, P., and Woods, D.L. (2002). Shape perception reduces activity in human primary visual cortex. Proc. Natl. Acad. Sci. U S A *99*, 15164–15169. https://doi.org/10.1073/pnas.192579399.

Nassi, J.J., and Callaway, E.M. (2009). Parallel processing strategies of the primate visual system. Nat. Rev. Neurosci. *10*, 360–372. https://doi.org/10.1038/nrn2619.

Nassi, J.J., Gómez-Laberge, C., Kreiman, G., and Born, R.T. (2014). Corticocortical feedback increases the spatial extent of normalization. Front Syst. Neurosci. *8*, 105. https://doi.org/10.3389/fnsys.2014.00105.

Nassi, J.J., Lomber, S.G., and Born, R.T. (2013). Corticocortical feedback contributes to surround suppression in V1 of the alert primate. J. Neurosci. *33*, 8504–8517. https://doi.org/10.1523/jneurosci.5124-12.2013.

Nauhaus, I., Busse, L., Carandini, M., and Ringach, D.L. (2009). Stimulus contrast modulates functional connectivity in visual cortex. Nat. Neurosci. *12*, 70–76.

Niemeyer, J.E., and Paradiso, M.A. (2016). Contrast sensitivity, V1 neural activity, and natural vision. J. Neurophysiol. *117*, 492–508.

Nitsche, M.A., and Paulus, W. (2000). Excitability changes induced in the human motor cortex by weak transcranial direct current stimulation. J. Physiol. *527*, 633–639.

Nitsche, M.A., and Paulus, W. (2001). Sustained excitability elevations induced by transcranial DC motor cortex stimulation in humans. Neurology *57*, 1899–1901. https://doi.org/10.1212/wnl.57.10.1899.

Nurminen, L., Merlin, S., Bijanzadeh, M., Federer, F., and Angelucci, A. (2018). Top-down feedback controls spatial summation and response amplitude in primate visual cortex. Nat. Commun. *9*, 2281. https://doi.org/10.1038/s41467-018-04500-5.

Olausson, B., Shyu, B.C., and Rydenhag, B. (1990). Properties of single neurons in the cat midsuprasylvian gyrus. Exp. Brain Res. *79*, 515–529. https://doi.org/10.1007/bf00229321.

Olson, C.R., and Lawler, K. (1987). Cortical and subcortical afferent connections of a posterior division of feline area 7 (area 7p). J. Comp. Neurol. *259*, 13–30. https://doi.org/10.1002/cne.902590103.

Padnick, L.B., and Linsenmeier, R.A. (1999). Properties of the flash visual evoked potential recorded in the cat primary visual cortex. Vis. Res. *39*, 2833–2840. https://doi.org/10.1016/S0042-6989(99)00016-4.

Pafundo, D.E., Nicholas, M.A., Zhang, R., and Kuhlman, S.J. (2016). Top-down-mediated facilitation in the visual cortex is gated by subcortical neuromodulation. J. Neurosci. *36*, 2904–2914. https://doi.org/10.1523/jneurosci.2909-15.2016.

Pak, A., Ryu, E., Li, C., and Chubykin, A.A. (2020). Top-down feedback controls the cortical representation of illusory contours in mouse primary visual cortex. J. Neurosci. *40*, 648–660. https://doi.org/10.1523/jneurosci.1998-19.2019.

Pan, D., Pan, H., Zhang, S., Yu, H., Ding, J., Ye, Z., and Hua, T. (2021a). Top-down influence affects the response adaptation of V1 neurons in cats. Brain Res. Bull. *167*, 89–98. https://doi.org/10.1016/j.brainresbull.2020.12.007.

Pan, H., Zhang, S., Pan, D., Ye, Z., Yu, H., Ding, J., Wang, Q., Sun, Q., and Hua, T. (2021b). Characterization of feedback neurons in the high-level visual cortical areas that project directly to the primary visual cortex in the cat. Front. Neuroanat. *14*. https://doi.org/10.3389/fnana.2020.616465.

Parisi, V., Miglior, S., Manni, G., Centofanti, M., and Bucci, M.G. (2006). Clinical ability of pattern electroretinograms and visual evoked potentials in detecting visual dysfunction in ocular hypertension and glaucoma. Ophthalmology *113*, 216–228. https://doi.org/10.1016/j.ophtha.2005.10.044.

Pascual-Leone, A., and Walsh, V. (2001). Fast backprojections from the motion to the primary visual area necessary for visual awareness. Science *292*, 510–512. https://doi.org/10.1126/science.1057099.

Ress, D., and Heeger, D.J. (2003). Neuronal correlates of perception in early visual cortex. Nat. Neurosci. *6*, 414–420. https://doi.org/10.1038/nn1024.

Richter, C.G., Coppola, R., and Bressler, S.L. (2018). Top-down beta oscillatory signaling conveys behavioral context in early visual cortex. Sci. Rep. *8*, 6991. https://doi.org/10.1038/s41598-018-25267-1.

Riesenhuber, M., and Poggio, T. (1999). Hierarchical models of object recognition in cortex. Nat. Neurosci. *2*, 1019–1025. https://doi.org/10.1038/14819.

Ro, T., Breitmeyer, B., Burton, P., Singhal, N.S., and Lane, D. (2003). Feedback contributions to visual awareness in human occipital cortex. Curr. Biol. *13*, 1038–1041.

Roebuck, H., Bourke, P., and Guo, K. (2014). Role of lateral and feedback connections in primary visual cortex in the processing of spatiotemporal regularity - a TMS study. Neuroscience *263*, 231–239. https://doi.org/10.1016/j.neuroscience.2014.01.027.

Roland, P.E., Hanazawa, A., Undeman, C., Eriksson, D., Tompa, T., Nakamura, H., Valentiniene, S., and Ahmed, B. (2006). Cortical feedback depolarization waves: a mechanism of top-down influence on early visual areas. Proc. Natl. Acad. Sci. U S A *103*, 12586–12591. https://doi.org/10.1073/pnas.0604925103.

Rolls, E.T. (2008). Top-down control of visual perception: attention in natural vision. Perception *37*, 333–354.

Schweid, L., Rushmore, R.J., and Valero-Cabre, A. (2008). Cathodal transcranial direct current stimulation on posterior parietal cortex disrupts visuo-spatial processing in the contralateral visual field. Exp. Brain Res. *186*, 409–417. https://doi.org/10.1007/s00221-007-1245-0.

Seidemann, E., and Geisler, W.S. (2018). Linking V1 activity to behavior. Annu. Rev. Vis. Sci. *4*, 287–310. https://doi.org/10.1146/annurev-vision-102016-061324.

Serre, T., Oliva, A., and Poggio, T. (2007). A feedforward architecture accounts for rapid categorization. Proc. Natl. Acad. Sci. U S A *104*, 6424–6429. https://doi.org/10.1073/pnas.0700622104.

Si, J., Zhang, X., Li, Y., Zhang, Y., Zuo, N., and Jiang, T. (2016). Correlation between electrical and hemodynamic responses during visual stimulation with graded contrasts. J. Biomed. Opt. *21*, 091315. https://doi.org/10.1117/1.jbo.21.9.091315.

Silvanto, J. (2014). Is primary visual cortex necessary for visual awareness? Trends Neurosci. *37*, 618–619. https://doi.org/10.1016/j.tins.2014.09.006.

Silvanto, J. (2015). Why is "blindsight" blind? A new perspective on primary visual cortex, recurrent activity and visual awareness. Conscious. Cogn. *32*, 15–32. https://doi.org/10.1016/j.concog.2014.08.001.

Silvanto, J., Cowey, A., Lavie, N., and Walsh, V. (2005a). Striate cortex (V1) activity gates awareness of motion. Nat. Neurosci. *8*, 143–144. https://doi.org/10.1038/nn1379.

Silvanto, J., Lavie, N., and Walsh, V. (2005b). Double dissociation of V1 and V5/MT activity in visual awareness. Cerebral Cortex *15*, 1736–1741. https://doi.org/10.1093/cercor/bhi050.

Slotnick, S.D. (2018). The experimental parameters that affect attentional modulation of the ERP C1 component. Cogn. Neurosci. *9*, 53–62. https://doi.org/10.1080/17588928.2017.1369021.

Souza, G.S., Gomes, B.D., Saito, C.A., da Silva Filho, M., and Silveira, L.C. (2007). Spatial luminance contrast sensitivity measured with transient VEP: comparison with psychophysics and evidence of multiple mechanisms. Invest. Ophthalmol. Vis. Sci. *48*, 3396–3404. https://doi.org/10.1167/iovs.07-0018.

Stagg, C.J., Bachtiar, V., and Johansen-Berg, H. (2011). The role of GABA in human motor learning. Curr. Biol. *21*, 480–484. https://doi.org/10.1016/j.cub.2011.01.069.

Stagg, C.J., Best, J.G., Stephenson, M.C., O'Shea, J., Wylezinska, M., Kincses, Z.T., Morris, P.G., Matthews, P.M., and Johansen-Berg, H. (2009). Polarity-sensitive modulation of cortical neurotransmitters by transcranial stimulation. J. Neurosci. *29*, 5202–5206. https://doi.org/10.1523/jneurosci.4432-08.2009.

Stoerig, P., and Cowey, A. (1995). Visual perception and phenomenal consciousness.

Behav. Brain Res. *71*, 147–156. https://doi.org/10.1016/0166-4328(95)00050-x.

Stoerig, P., and Cowey, A. (2007). Blindsight. Curr. Biol. *17*, R822–R824.

Thiele, A., Pooresmaeili, A., Delicato, L.S., Herrero, J.L., and Roelfsema, P.R. (2009). Additive effects of attention and stimulus contrast in primary visual cortex. Cereb. Cortex *19*, 2970–2981. https://doi.org/10.1093/cercor/bhp070.

Tokashiki, N., Nishiguchi, K.M., Fujita, K., Sato, K., Nakagawa, Y., and Nakazawa, T. (2018). Reliable detection of low visual acuity in mice with pattern visually evoked potentials. Sci. Rep. *8*, 15948. https://doi.org/10.1038/s41598-018-34413-8.

Tomiyama, Y., Fujita, K., Nishiguchi, K.M., Tokashiki, N., Daigaku, R., Tabata, K., Sugano, E., Tomita, H., and Nakazawa, T. (2016). Measurement of electroretinograms and visually evoked potentials in awake moving mice. PLoS One *11*. e0156927. https://doi.org/10.1371/journal.pone.0156927.

Tong, F. (2003). Primary visual cortex and visual awareness. Nat. Rev. Neurosci. *4*, 219–229. https://doi.org/10.1038/nrn1055.

Tong, L., Zhu, B., Li, Z., Shou, T., and Yu, H. (2011). Feedback from area 21a influences orientation but not direction maps in the primary visual cortex of the cat. Neurosci. Lett. *504*, 141–145. https://doi.org/10.1016/j.neulet.2011.09.019.

van Kleef, J.P., Cloherty, S.L., and Ibbotson, M.R. (2010). Complex cell receptive fields: evidence for a hierarchical mechanism. J. Physiol. *588*, 3457–3470. https://doi.org/10.1113/jphysiol.2010.191452.

van Loon, A.M., Fahrenfort, J.J., van der Velde, B., Lirk, P.B., Vulink, N.C.C., Hollmann, M.W., Steven Scholte, H., and Lamme, V.A.F. (2015). NMDA receptor antagonist ketamine distorts object recognition by reducing feedback to early visual cortex. Cereb. Cortex *26*, 1986–1996. https://doi.org/10.1093/cercor/bhv018.

Vandenbussche, E., and Orban, G.A. (1983). Meridional variations in the line orientation discrimination of the cat. Behav. Brain Res. *9*, 237–255.

Wang, C., Huang, J.Y., Bardy, C., FitzGibbon, T., and Dreher, B. (2010). Influence of 'feedback' signals on spatial integration in receptive fields of cat area 17 neurons. Brain Res. *1328*, 34–48. https://doi.org/10.1016/j.brainres.2010.02.069.

Wang, C., Rajagovindan, R., Han, S.-M., and Ding, M. (2016). Top-down control of visual alpha oscillations: sources of control signals and their mechanisms of action. Front. Hum. Neurosci. *10*, 15. https://doi.org/10.3389/fnhum.2016.00015.

Wang, C., Waleszczyk, W.J., Burke, W., and Dreher, B. (2000). Modulatory influence of feedback projections from area 21a on neuronal activities in striate cortex of the cat. Cereb. Cortex *10*, 1217–1232.

Wang, C., Waleszczyk, W.J., Burke, W., and Dreher, B. (2007). Feedback signals from cat's area 21a enhance orientation selectivity of area 17 neurons. Exp. Brain Res. *182*, 479–490. https://doi.org/10.1007/s00221-007-1014-0.

Wang, M., Arteaga, D., and He, B.J. (2013). Brain mechanisms for simple perception and bistable perception. Proc. Natl. Acad. Sci. U S A *110*, E3350–E3359. https://doi.org/10.1073/pnas.1221945110.

Whittingstall, K., Wilson, D., Schmidt, M., and Stroink, G. (2008). Correspondence of visual evoked potentials with FMRI signals in human visual cortex. Brain Topography *21*, 86–92. https://doi.org/10.1007/s10548-008-0069-y.

Williford, T., and Maunsell, J.H.R. (2006). Effects of spatial attention on contrast response functions in macaque area V4. J. Neurophysiol. *96*, 40–54. https://doi.org/10.1152/jn.01207.2005.

Wilson, T.W., McDermott, T.J., Mills, M.S., Coolidge, N.M., and Heinrichs-Graham, E. (2018). tDCS modulates visual gamma oscillations and basal alpha activity in occipital cortices: evidence from MEG. Cereb. Cortex *28*, 1597–1609. https://doi.org/10.1093/cercor/bhx055.

Wong, C., Pearson, K.G., and Lomber, S.G. (2018). Contributions of parietal cortex to the working memory of an obstacle acquired visually or tactilely in the locomoting cat. Cerebral Cortex *28*, 3143–3158. https://doi.org/10.1093/cercor/bhx186.

Yang, J., Wang, Q., He, F., Ding, Y., Sun, Q., Hua, T., and Xi, M. (2016a). Dietary restriction affects neuronal response property and GABA synthesis in the primary visual cortex. PLoS One *11*. e0149004. https://doi.org/10.1371/journal.pone.0149004.

Yang, X., Ding, H., and Lu, J. (2016b). Feedback from visual cortical area 7 to areas 17 and 18 in cats: how neural web is woven during feedback. Neuroscience *312*, 190–200. https://doi.org/10.1016/j.neuroscience.2015.11.015.

Zhang, G.L., Li, H., Song, Y., and Yu, C. (2015). ERP C1 is top-down modulated by orientation perceptual learning. J. Vis. *15*, 8. https://doi.org/10.1167/15.10.8.

Zhang, S., Xu, M., Kamigaki, T., Hoang Do, J.P., Chang, W.C., Jenvay, S., Miyamichi, K., Luo, L., and Dan, Y. (2014). Selective attention. Long-range and local circuits for top-down modulation of visual cortex processing. Science *345*, 660–665. https://doi.org/10.1126/science.1254126.

Zhao, X., Ding, J., Pan, H., Zhang, S., Pan, D., Yu, H., Ye, Z., and Hua, T. (2020). Anodal and cathodal tDCS modulate neural activity and selectively affect GABA and glutamate syntheses in the visual cortex of cats. J. Physiol. *598*, 3727–3745. https://doi.org/10.1113/jp279340.

Zhou, Y., Huang, C., Xu, P., Tao, L., Qiu, Z., Li, X., and Lu, Z.L. (2006). Perceptual learning improves contrast sensitivity and visual acuity in adults with anisometropic amblyopia. Vis. Res *46*, 739–750.

STAR★METHODS

KEY RESOURCES TABLE

REAGENT or RESOURCE	SOURCE	IDENTIFIER
Deposited data		
Data by figure	Mendeley Dataset	https://www.dx.doi.org/10.17632/ysbjtgrg2p.1
Software and algorithms		
Matlab R2014a	Mathworks	https://www.mathworks.com/products/matlab.html, RRID:SCR_001622
Psychtoolbox 2.54	(Brainard, 1997)	http://psychtoolbox.org/, RRID:SCR_002881
Igor Pro 6.54	WaveMetrics, Inc.	http://www.wavemetrics.com/products/igorpro/igorpro.htm, RRID:SCR_000325
SPSS 13.0	IBM Corp., Armonk, N.Y., USA	https://www.ibm.com/products/spss-statistics, RRID:SCR_019096
Matlab and Igor code	Mendeley Dataset	https://www.dx.doi.org/10.17632/ysbjtgrg2p.1

RESOURCE AVAILABILITY

Lead contact

Further information and requests for resources should be directed to and will be fulfilled by the lead contact Z-L Lu (zhonglin@nyu.edu).

Materials availability

This study did not generate new specimens or materials. All images are included in the text and supplemental information.

Data and code availability

- All original dataset has been deposited at Mendeley Data and are publicly available as of the date of publication. The DOI is listed in the key resources table.
- All original code has been deposited at Mendeley Data and is publicly available as of the date of publication. The DOI are listed in the key resources table.
- Any additional information required to reanalyze the data reported in this paper is available from the lead contact upon request.

EXPERIMENTAL MODEL AND SUBJECT DETAILS

Seven young adult male cats (age 2–5 years, body weight 2.7–4.2 kg) were used in this study. Four of them were randomly selected to evaluate tDCS-induced top-down influence on neuronal activity in V1. The other three were used in the experiment for behavioral and neuronal contrast sensitivity measurement before and after tDCS. All subjects were purchased from Nanjing Qing-Long-Shan Animal Breeding Farm (Jiangning District of Nanjing, Certificate No. SX1207), and all of them were disease-free, healthy cats with no optical or retinal abnormality. All animals were reared in rooms separated by transparent glass walls. Each room had comfortably organized living, feeding and playing areas with the room temperature maintained at 25°C. All experiments in this study were performed strictly in accordance with the National Institutes of Health Guide for the Care and Use of Laboratory Animals, and conformed to the principles and regulations as described in the ARRIVE guidelines (Animal Research: Reporting of In *Vivo* Experiments). All experiments and animal treatments were approved by the Ethics Committee of Anhui Normal University (approval NO. NS2017001).

METHOD DETAILS

Preparation for VEP recording in V1 cortex

The preparation for recording of visual evoked field potentials (VEPs) in V1 was performed with the following procedures according to previous studies (Hua et al., 2006, 2010; Meng et al., 2013; Yang et al., 2016a; Zhao et al., 2020). The cat was first anesthetized with ketamine HCl (40 mg/kg, im) and xylazine (2 mg/kg, im). Noninvasive intubation of tracheal and intravenous cannula was performed under sterile preparation. After the cat was fixed in a stereotaxic apparatus, glucose (5%)-saline (0.9%) solution containing a mixture of urethane (20 mg/kg body weight) and gallamine triethiodide (10 mg/kg body weight) was infused intravenously to maintain necessary anesthesia and paralysis. Artificial respiration was performed, and the expired pCO2 was kept at approximately 3.8%. Heart rate (approximately 180-220 pulses/min) and electrocardiogram were monitored throughout the experiment to assess the level of anesthesia and ensure that the animals were not responding to pain. The body temperature (38°C) was maintained using a heating blanket. Pupils were maximally dilated with atropine (0.5%). Artificial tear was applied to protect the cornea.

After tDCS chamber implantation in the higher-level cortex (A7&A5 or A7), a small hole (4 × 3 mm) was drilled on the skull over the central V1 area (Horsley–Clarke coordinates: P2-6/L2-4) of the left hemisphere. A chloride (Ag/AgCl) silver wire electrode (extending from P2 to P6, with an impedance of 0.3–0.5 MΩ) was placed on the surface of the dura over V1 area for VEP recording. The small hole was sealed with tissue adhesive after filling it with 4% agar. At the end of VEP recording in behavioral cats, the small hole on the skull over V1 was cleaned with saline, covered with absorbable gelfoam, and then sealed with bone wax. Intravenous infusion was terminated first, and artificial ventilation was disconnected once the animal recovered spontaneous breathing. The animal was sent to the nest after receiving a shot (1 mL) of antibiotic (800,000 units penicillin). Full care was given to the animal in the following week till complete recovery.

Administration of transcranial direct current stimulation

Before VEP recording or behavioral measurement, 3D-printed plastic rectangle-shaped chambers (8 × 6 × 10 mm) were implanted respectively on the skull over A7 (Horsley-Clarke coordinates: A0-A8/L6-L12) and A5 (A11-A19/L6-L12) or only A7 (in behavioral cats) (Avendaño et al., 1988; Galuske et al., 2002; Han et al., 2008; Lajoie et al., 2010; Olausson et al., 1990; Wong et al., 2018) of the left hemisphere using dental cement. The surgery was performed after the animals were anesthetized and maintained in normal physiological state with noninvasive artificial respiration and intravenous infusion as described above. At the end of the surgery for behavioral cats, all incisions around the trauma were closed and sutured, and the animals received full care in the subsequent two weeks. Antibiotic (*penicillin*, 800,000 units per day) was administered for about 2-3 days as needed. Behavioral measurement and VEPs recording in V1 cortex began after the cats recovered completely from the trauma.

tDCS was administered with an HD-tDCS stimulator (Soterix Medical, USA). A metal pin-type electrode (cathode) was placed in the tDCS chamber filled with 0.9% saline for conductance. The reference electrode (saline-soaked rubber electrode, 3 × 3 cm) was placed on the dorsal central neck skin after the hair over the intended site was clipped and cleaned with alcohol swabs. The output current intensity was maintained at 1 mA. At the onset and offset of stimulation, current was slowly ramped up and down over about 15 s to avoid sudden current change (Nitsche and Paulus, 2000; Schweid et al., 2008; Wilson et al., 2018; Zhao et al., 2020). For s-tDCS, the tDCS current was ramped down to zero after ramping up at the onset of stimulation, but ramped up and ramped down again at the end of sham stimulation. The application of different tDCS conditions (c- and s-tDCS in A7, c-tDCS in A5) was performed in a pseudorandom order in each cat. Because previous studies reported that tDCS-induced effects lasted for 60-90 min (Bachtiar et al., 2015; Monte-Silva et al., 2010; Nitsche and Paulus, 2001; Stagg et al., 2009, 2011; Zhao et al., 2020), we set the time interval between tDCS sessions at least 90 min. The duration of each tDCS session was 15 min.

Psychophysical measurement of behavioral contrast sensitivity

Conditioning training. Three adult male cats (age of 3-5 years, body weight of 3.4–4.2 kg) were used in this experiment. The behavior training equipment contained a PC computer for visual stimuli generation and presentation, left and right nose keys for the two-alternative forced choice task and a food reward pipe that was gated by an electric valve and automatically controlled by a custom-made electric circuit (De Weerd et al., 1990; Hua et al., 2010; Meng et al., 2013; Vandenbussche and Orban, 1983). Cats were

trained to identify the orientation of a vertically- or horizontally-oriented grating on the display by touching the left (for vertical gratings) or right (for horizontal gratings) nose key to get fish mush reward (Supplemental videos/Video S1). During conditioning training, the vertical or horizontal grating stimuli had a fixed spatial frequency (SF) of 0.4 cycle/deg and a fixed contrast of 100%. Each cat performed 640-800 trials per day, arranged in 8-10 training blocks. Each block contained 80 trials, with a 2-min resting period between blocks. The conditioning training ended after ≥90% correct performance was reached.

Measurement of behavioral CSF and TvC functions. To assess top-down influence of A7 on the behavioral contrast sensitivity function, we measured the cats' contrast thresholds in identifying vertical versus horizontal grating stimuli over a range of spatial frequencies (SF: 0.1, 0.2, 0.4, 0.6, 0.8 and 1.2 cycle/deg) (Figure S1A) using a 3-down/1-up staircase (d' = 1.634) method (Dosher and Lu, 1999; Zhou et al., 2006) before and after c- or s-tDCS in A7 (Figure S1B, Video S1). Eight daily CSF assessments, with 30 trials at each SF conditions in a pseudorandom order, were completed within 15 min both before and after tDCS. The estimated contrast thresholds from the previous day were used as initial contrasts in the staircase procedure. The average value of 1/threshold (mean ± SD) across eight repeated measurements was used to construct the CSF before and after c- and s-tDCS in A7.

To identify mechanisms of top-down influence on perceptual contrast sensitivity, we also measured the TvC function with increasing amounts of external noise (0, 0.04, 0.08, 0.16 and 0.32) (Figure S1C) before and after c- or s-tDCS in A7. The SF of the grating stimuli was fixed at 0.2 cycle/deg (near the optimal SF on the CSF). Twelve daily TvC measurements, with 30 trials at each of the five external noise conditions in a pseudorandom order (Figure S1D, Supplemental videos/Video S2), were completed using either a 2-down/1-up (d' = 1.089) or a 3-down/1-up (d' = 1.634) staircase procedure within 13 min both before and after tDCS. The average threshold values (mean ± SD) across six repeated sessions at each noise level was used to construct the TvC functions at the two performance criterion levels before and after c- and s-tDCS in A7.

At the end of each daily measurement, the cats were provided with supplemental ordinary food according to the food requirement during conditioning training.

Visual stimuli and display. Visual stimuli used in the conditioning training and psychophysical measurements included windowed sinusoidal gratings and external noise images (Figures S1A–S1C). All grating stimuli were generated in real time by a PC computer running MATLAB programs with Psychotoolbox extensions (Brainard, 1997), and were displayed on a CRT (resolution 1024 × 768 pixels, refresh rate 75 Hz) positioned 57 cm from the animal's eyes. The grating stimuli oriented vertically or horizontally, extended 8° in radius, and had a fixed mean luminance of 19 cd/m^2. The orientation of the grating was randomly selected in each trial and presented with an inter-trial interval of 2.5 s. The duration of each grating presentation was 2.35 s, including a denied period (RDP) of 0.35s during which nose key touch triggered no food reward. Before each stimulus presentation, a flashing dot (0.2°C × 0.2°C) was displayed at the center of the CRT as a cue for the cat to fixate. Because large-size grating stimuli (8° in radius at 57 cm viewing distance) were used in this study, eye fixation was not important and was not monitored.

In the TvC measurements, visual stimuli were composed of external noise and signal frames (Figure S1C). The external noise frames had the same size as that of the signal frames with each noise element subtending 2 × 2 pixel or 0.024°C × 0.024°C. The graylevels of the noise elements in each external noise frame were drawn independently from a Gaussian distribution with mean 0 and standard deviation corresponding to the external noise condition. To guarantee that the external noise did conform to the Gaussian distribution, the maximum standard deviation of the noise was kept below 33% maximum achievable contrast. Five external noise levels (0.00, 0.04, 0.08, 0.16 and 0.32) were used in the experiment.

VEP recording and visual stimuli

VEP signals in V1 cortex were recorded with the embedded silver wire electrode. Signals were amplified with a microelectrode amplifier (Dagan 2400A, USA) (gain 1000, band-pass filtered between 1 and 100 Hz). Visual stimuli were generated by a PC computer using MATLAB programs based on Psychotoolbox extensions (Brainard, 1997), and were presented on a CRT (resolution 1024 × 768 pixels, refresh rate 75 Hz) positioned 57 cm from the animal's eyes.

Examination of top-down influence on neuronal activity in V1. To evaluate whether and how top-down influence of A7 affects neuronal activity in V1, we recorded VEPs in V1 cortex in response to horizontal sinusoidal grating stimuli (full screen size, with 0.2 cycle/deg spatial frequency, 2 Hz temporal frequency and 100% contrast) before and after c- and s-tDCS in A7 as well as c-tDCS in A5 of the non-visual parietal cortex. The application of different tDCS conditions were performed in a pseudorandom order with an interval of at least 90 min. We repeated 6 recording sessions (each with 3 different tDCS conditions) in each cat. For each tDCS condition, the VEPs were recorded repeatedly before and at different time points (0-90 min, with a 10-min interval) after tDCS. Data collection at each time point consisted of 30 trials of visual stimulus presentation. .

Examination of neuronal contrast sensitivity in V1. *Visual stimuli* Because VEP provides measures of neuronal population activities that exhibit similar preferences for stimulus orientation, direction of motion, contrast and size as single-unit activities (Kayser and König, 2004; Lashgari et al., 2012) and are closely related to visual perception (Kayser and König, 2004; Souza et al., 2007), we evaluate neuronal contrast sensitivity changes in the V1 cortex of behavioral cats based on VEPs recorded before and after tDCS in A7. The c- and s-tDCS were applied in a pseudorandom order with an interval of at least 90 min (Zhao et al., 2020) and repeated 6 sessions in each cat. VEPs were elicited by horizontally moving grating stimuli (with an 8° diameter size and 8 Hz temporal frequency) with varied luminance contrasts (0, 0.05, 0.1, 0.2, 0.3, 0.4, 0.5, 0.6, 0.8 and 1.0) at different SFs (0.1, 0.2, 0.4, 0.6, 0.8 and 1.2 c/deg) or moving grating stimuli (at fixed SF of 0.2 cycle/deg, near optimal SF) with gradient luminance contrasts at different external noise levels (0.00, 0.04, 0.08, 0.16 and 0.32) generated by adding external noise images to sinusoidal gratings as described above (Figure S1C) except that the grating and noise images were moving in the same direction. All grating stimuli and noise images were displayed on the CRT (resolution: 1024 × 768 pixels, refresh rate: 75 Hz) positioned 57 cm from the animal's eyes. The duration of each stimulus presentation was 0.4 s, and baseline VEPs were acquired during a 0.3 s pre-stimulus interval in which the still grating image was shown on the CRT.

Measurement of neuronal CSF and TvC functions Neuronal CSF and TvC functions in each behavioral cat were measured separately on different days by recording VEPs on V1 cortex in response to grating stimuli with gradient contrasts in different SF conditions and at different external noise levels, respectively. The c-tDCS and s-tDCS in A7 were performed in an interleaved sequence and repeated 6 sessions. For each tDCS session, VEPs recordings in different SF conditions or at different external noise levels were interleaved and repeated 4 iterations. In each iteration, VEP recordings in different stimulus contrasts were randomized and repeated for 5 trials in each SF or external noise condition. The recordings in each session were completed within 15 min both before and after tDCS.

QUANTIFICATION AND STATISTICAL ANALYSIS

Evaluation of top-down influence on neuronal activity in V1

VEP signals were averaged across the 30 trials and filtered (60 Hz notch filter, 1-100 Hz bandpass) (Aydin-Abidin et al., 2006; Bao et al., 2010; Geisler and Albrecht, 1997; Zhao et al., 2020) using Igor (see key resources table). Peak latency of N1, P1 and N2 components and peak-to-peak amplitude of N1P1 (the absolute amplitude from the peak of N1 to the peak of P1) and P1N2 (the absolute amplitude from the peak of P1 to the peak of N2) were extracted (Figures 1A–1C) according to previous studies (Aydin-Abidin et al., 2006; Ding et al., 2016; Souza et al., 2007; Zhao et al., 2020). The average latency and amplitude of VEPs recorded before and at different time (0-90 min, with a 10-min interval) after tDCS were expressed as mean ± SD. Statistical comparisons of mean latency and amplitude of VEPs recorded before and at different measurement time after (time point: n = 11) c- and s-tDCS in A7 as well as c-tDCS in A5 (tDCS condition: n = 3) were conducted with ANOVA (in Figures 1D–1F and results) and *post hoc* tests (in Figures 1E and 1F and results) using SPSS (see key resources table).

Construct neuronal CSF and TvC functions with ROC analysis

The VEP signals evoked by a stimulus with each signal contrast at each stimulus SF or at each external noise level before or after tDCS were averaged every 30 trials, and then filtered (1-100 Hz band-pass, 60 Hz notch filter) to measure the peak-to-peak amplitudes of the N1P1 and P1N2 (Aydin-Abidin et al., 2006; Ding et al., 2016; Souza et al., 2007; Zhao et al., 2020) using Igor (Figures S2/M1 and S3). Because VEP amplitudes are fine-tuned to stimulus contrast (Hood et al., 2006; Souza et al., 2007), we estimated the neuronal threshold

contrast (TC) using the Receiver Operating Characteristics (ROC) analysis in MATLAB (see key resources table) based on the distributions of VEP amplitudes in different stimulus conditions (Adab and Vogels, 2011; Edwards et al., 1995; Parisi et al., 2006). The VEP amplitude distribution in each stimulus condition was constructed by estimating the VEP amplitude 500 times, each based on a random selection of 30 trials (10 trials/session) from 3 out of 6 recording sessions (Figures S2/M2 and S3). We obtained 20 VEP amplitude distributions in each stimulus condition based on random selection of 3 out of 6 recording sessions. These VEP amplitude distribution at different stimulus contrasts were respectively compared with the baseline (zero signal contrast in the same external noise condition) in a standard ROC analysis to compute the area under the curve, that is, the accuracy in making signal-present or signal-absent decisions (Figures S2/M3 and S3). The neurometric function in each external noise condition was then constructed by plotting detection probability as a function of signal contrast. Neuronal threshold contrasts (TCs) corresponding to 70.7% ($d_1' = 1.089$) and 79.4% ($d_2' = 1.634$) detection accuracy in each stimulus condition were then estimated from the neurometric function. The whole computation procedure was performed for 20 repetitions to obtain standard deviations of the TCs (Figures S2/M4 and S3). The means of the inverted TCs across the 20 repetitions were used to construct pre- and post-tDCS CSF functions, and the mean TCs across 20 repetitions in different external noise conditions were used to construct pre- and post-tDCS TvC functions. All value were expressed as mean ± SD.

Comparisons of behavioral and neuronal CSF and TvC functions

Comparisons of behavioral and neuronal CSF and TvC functions were performed using SPSS (see key resources table). The mean behavioral and V1 neuronal contrast sensitivity (CS) at different stimulus SFs (SF level: n = 6) before and after c- or s-tDCS in A7 was compared using two-factor ANOVA and *post hoc* tests (in Figures 2 and 3 and results). The difference between behavioral CS reductions and N1P1- or P1N2-neuronal CS reductions at 0.1, 0.2, 0.4 and 0.6 cycle/deg (SF level: n = 4) after c-tDCS was compared with two-factor ANOVA (in results). The mean behavioral and V1 neuronal threshold contrast (TC) measured at different external noise levels (noise level: n = 5) under two performance criteria (n = 2) before and after c- or s-tDCS in A7 was compared using three-factor ANOVA (in Figures 5 and 6 and results). The difference between behavioral TC increase and N1P1- or P1N2-neuronal TC increase at different external noise levels (noise level: n = 5) after c-tDCS was compared with two-factor ANOVA (in results). The relationship between behavioral and neuronal CSFs (SF level: n = 6) or TvCs (noise level: n = 5) before and after c-tDCS in A7 was assessed with pearson correlation test (in Figures 4 and 7 and results).

PTM modeling analysis

In order to quantify top-down effect of A7 on neuronal contrast sensitivity in V1 and cats' behavior in contrast detection, we fit the Perceptual Template Model (PTM) (Dosher and Lu, 1999; Lu and Dosher, 1998) to the pre- and post-tDCS behavioral and neuronal TvC functions, respectively. The PTM has been used to identify mechanisms of performance improvements in attention (Dosher and Lu, 2000a; Lu and Dosher, 1998, 2004) and perceptual learning (Dosher and Lu, 1999; Huang et al., 2008; Lu et al., 2005; Zhou et al., 2006). A least square procedure was used to fit the PTM to the neuronal and behavioral TvC functions:

$$C_\tau = \frac{1}{\beta}\left[\frac{\left(1+(A_m N_m)^2\right)(A_f N_{ext})^{2\gamma}+(A_a N_a)^2}{1/(d')^2-(A_m N_m)^2}\right]^{\frac{2\gamma}{\gamma}}, \qquad \text{(Equation 1)}$$

where C_τ represents threshold contrast at the d' performance level, N_a denotes the standard deviation of internal additive noise, N_{ext} denotes the standard deviation of external noise, N_m denotes the proportional constant of multiplicative noise, β denotes the gain of the perceptual template, and γ denotes the exponent of the non-linear transducer. A_a, A_f and A_m were set to 1.0 for TvCs before c-tDCS, and were free to vary for TvCs after c-tDCS.

The fit was performed in MATLAB (2014a) (see key resources table) with the curvefit toolbox extension. The sum of the squared differences between the measured and model-predicted log thresholds was minimized. The goodness of fit (in Table 1 and results) was determined by:

$$r^2 = 1.0 - \frac{\sum\left[\log\left(C_\tau^{predict}\right)-\log(C_\tau)\right]^2}{\sum\{\log(C_\tau)-\text{mean}[\log(C_\tau)]\}^2}, \qquad \text{(Equation 2)}$$

An F statistic was used to compare nested models (in Tables 1, 2 and results):

$$F(df_1, df_2) = \frac{(r^2_{full} - r^2_{reduced})/df_1}{(1 - r^2_{full})/df_2} \quad \text{(Equation 3)}$$

where $df_1 = k_{full} - k_{reduced}$ and $df_2 = N - k_{full}$; N is the number of predicted data points.

The standard deviation of each model parameter for the best-fitting model was estimated with a bootstrap method (Dosher et al., 2013; Huang et al., 2009; Jeon et al., 2014; Zhou et al., 2006). In brief, the contrast threshold at a given external noise level was assumed to have a Gaussian distribution with its mean equal to the mean threshold of all the observers and the standard deviation estimated from inter-observer variability. The bootstrap procedure was used to generate 1000 pairs of resampled TvC functions based on the mean and standard deviation of the observed data, corresponding to the 2-down/1-up ($d_1' = 1.089$) and 3-down/1-up staircases ($d_2' = 1.634$), for each cat before and after tDCS. By fitting the PTM to these resampled TvC functions, the mean and standard deviation of the best-fitting model parameters were obtained (in Table 1 and results).